Heini Saloniemi

Electrodeposition of PbS, PbSe and PbTe thin films
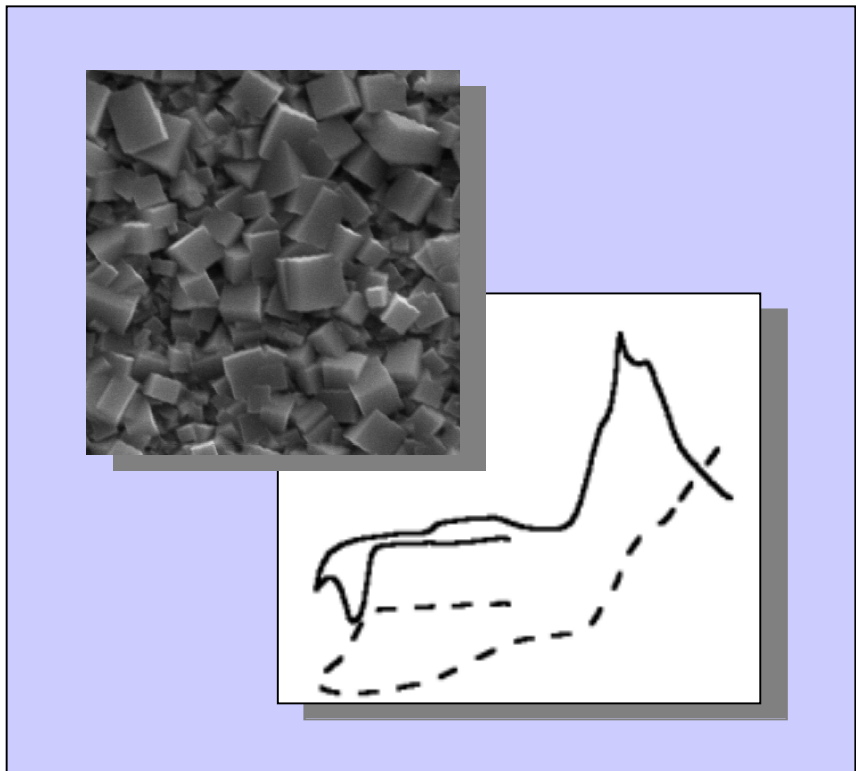
Electrodeposition of PbS, PbSe and PbTe thin films

Heini Saloniemi

Laboratory of Inorganic Chemistry
Department of Chemistry
Faculty of Science
University of Helsinki

Academic dissertation

To be presented, with the permission of the Faculty of Science of the University of Helsinki, for public criticism in Auditorium A110 of the Department of Chemistry on December 15, 2000, at 12 noon.

Abstract

Lead chalcogenides (PbS, PbSe, PbTe) are narrow band gap semiconductors which are largely used in infrared applications. In the present study lead chalcogenide thin films were deposited electrochemically from aqueous solutions. Two different electrodeposition methods were used; PbSe and PbTe thin films were prepared at constant potential while PbS was deposited by cycling the potential.

Chemical and physical properties of the films were examined by various techniques, and their electrical properties were studied as well. PbSe and PbS thin films were found to be stoichiometric whereas PbTe thin films contained an excess of Te. The films contained water as an impurity. All the films had polycrystalline, randomly oriented cubic structure. After annealing the films showed p-type conductivity. The annealing at 100 °C did not affect much the resistivities of PbS and PbTe which remained between 0.5–10 Ω cm but the resistivity of PbSe films increased to 1–60 kΩ cm. All films showed IR activity.

Electrodeposition mechanisms of PbSe, PbTe and PbS thin films and electrochemistry of the related precursors were studied by means of the electrochemical quartz crystal microbalance (EQCM) combined with cyclic voltammetry. Both film growth and EQCM studies showed that the electrodeposition of PbSe and PbTe occurs by the induced codeposition mechanism, where Se (or Te) is deposited first and induces the reduction of lead ions to form PbSe (or PbTe) so that this occurs at more positive potential than where lead alone would be deposited. Electrodeposition of PbS, on the other hand, turned out to be complicated including several simultaneous processes.

Preface

This thesis is based on the experimental work carried out during the 1996–2000 in the Laboratory of Inorganic Chemistry at the Department of Chemistry at the University of Helsinki.

I wish to express my deep gratitude to excellent supervisors Professor Markku Leskelä and Docent Mikko Ritala for their invaluable advice and guidance.

I am thankful to all my coworkers, especially to Ms. Marianna Kemell, who has fight along with me during the last few years in the laboratory. Mr. Tapio Kanniainen, Prof. Reijo Lappalainen, Prof. Jouko Vähäkangas, Dr. Pentti Niemelä and Mr. Raimo Rikola are also acknowledged for contributing this project.

I want to thank my roommate Ms. Marika Juppo, all staff in the Laboratory of Inorganic Chemistry, and of course The Hot Guys, The Film Masters, for good moments and nice time also outside the laboratory.

I would like to thank my dear friend Eva for her support and empathy, I will never forget our invaluable emergency meetings, and Maaret, for taking care of also my physical condition.

I wish to thank my parents Riitta and Tuomo, and my brothers and sister, for their continuous support.

Finally, I would like to thank my dearest Mikko again, for his love, encouragement and enormous patience also at home.

List of publications

This work is based on the following original publications which are referred in the text by their Roman numerals. In addition, the electrical properties of the PbS, PbSe and PbTe thin films are discussed on the basis of unpublished results.

I Saloniemi, H., Kanniainen, T., Ritala, M., Leskelä, M. and Lappalainen, R. Electrodeposition of lead selenide thin films. J. Mater. Chem., 8 (1998), p. 651.

II Saloniemi, H., Kanniainen, T., Ritala, M. and Leskelä, M. Electrodeposition of PbTe thin films. Thin Solid Films, 326 (1998), p. 78.

III Saloniemi, H., Ritala, M., Leskelä, M. and Lappalainen, R. Cyclic electrodeposition of PbS thin films. J. Electrochem. Soc., 146 (1999), p. 2522.

IV Saloniemi, H., Kemell, M., Ritala, M. and Leskelä, M. Electrochemical quartz crystal microbalance and cyclic voltammetry studies on PbSe electrodeposition mechanisms. J. Mater. Chem. 10 (2000), p. 519.

V Saloniemi, H., Kemell, M., Ritala, M. and Leskelä, M. PbTe electrodeposition studied by combined electrochemical quartz crystal microbalance and cyclic voltammetry. J. Electroanal. Chem., 482 (2000), p. 139.

VI Saloniemi, H., Kemell, M., Ritala, M. and Leskelä, M. Electrochemical quartz crystal microbalance study on cyclic electrodeposition of PbS thin films. Thin Solid Films, submitted.

The author has written all the articles and done most of the experimental work, including thin film growth experiments, cyclic voltammetry and EQCM analysis, XRD, SEM, EDX, profilometry, hot point probe and four point probe measurements. Ion beam analyses were done in the Accelerator Laboratory at the Department of Physics at the University of Helsinki, WDX analysis at Geological Survey of Finland and some of the electrical measurements at VTT Electronics and Rikola ltd both in Oulu.

Contents

Appendices of this publication are not included in the PDF version. Please order the printed version to get the complete publication (http://otatrip.hut.fi/vtt/jure/index.html)

List of symbols and abbreviations

a	activity
A	surface area
ALE	atomic layer epitaxy
CBD	chemical bath deposition
CVD	chemical vapour deposition
D*	detectivity
DEG	diethylene glycol
DMF	dimethyl formamide
DMSO	dimethylsulfoxide
E	potential
E°	standard potential
E_g	band gap
ECALE	electrochemical atomic layer epitaxy
EDTA	ethylenediaminetetraacetic acid
EDX	energy dispersive X-ray analysis
EG	ethylene glycol
ERDA	elastic recoil detection analysis
EQCM	electrochemical quartz crystal microbalance
f	frequency
f_0	resonant frequency
F	Faraday constant (96485 C mol^{-1})
FA	formaldehyde
G	Gibbs free energy
HWE	hot wall epitaxy
I	current
IR	infrared
m	mass

M	molar mass
MOCVD	metalorganic chemical vapour deposition
n	number of moles
NTA	nitrilotriacetic acid
PG	propylene glycol
Q	charge
QCM	quartz crystal microbalance
R	gas constant (8.315 J $(K\ mol)^{-1}$) or resistance
$R_\square$	sheet resistance
RBS	Rutherford backscattering spectroscopy
RT	room temperature
SEM	scanning electron microscopy
SHE	standard hydrogen electrode
SILAR	successive ionic layer adsorption and reaction
T	temperature
TOF-ERDA	time-of-flight elastic recoil detection analysis
UPD	under potential deposition
WDX	wavelength dispersive X-ray analysis
XRD	X-ray diffraction
z	number of electrons (involved in an electrochemical reaction)
β	stability constant
μ	shear modulus
ρ	density
τ	time constant
λ	wavelength

1. Introduction

Electrodeposition is more than 150 years old thin film preparation technique which has largely been used to deposit metal films. [1] In addition, during the last twenty five years electrodeposition has been more intensively studied in preparing compound semiconductors. In comparison with other techniques, electrodeposition is relatively easily scalable and cost effective as it is a nonvacuum, room temperature method. In addition, substrates with various sizes and shapes may be used and toxic gaseous precursors are not needed unlike in many gas phase techniques. In comparison with chemical bath deposition, which is the other common liquid phase film deposition technique, electrodeposition processes are more easily controllable since the film compositions are not very sensitive to small variations in the precursor concentrations and the precursor solutions are stable.

Lead chalcogenides (PbS and PbSe) have been used for forty years in academic, commercial and military infrared (IR) applications, including spectrometer detectors, flame detection, pollution monitor and night vision systems. In addition, PbTe has been investigated for example due to its thermoelectric properties.

The purpose of this work was to study the preparation of PbSe, PbTe and PbS thin films by electrodeposition and find suitable, mild, aqueous deposition conditions for reproducible film growth. The aim was to apply the induced codeposition method, which is best known from CdTe electrodeposition studies, for PbSe and PbTe and to find conditions where PbS films could be deposited from a more stable precursor solution than those used before. In addition, electrodeposition mechanisms of the lead chalcogenides were investigated for the first time in more detail by means of an electrochemical quartz crystal microbalance combined with cyclic voltammetry. The electrical properties of the electrodeposited lead chalcogenide films, which have not been reported earlier, were measured from two types of devices, photoconductors and photovoltaic diodes.

The present thesis gives at first an introduction to the electrodeposition in general, and the electrodeposition of chalcogenide (sulfide, selenide and telluride) compounds in particular. As the cadmium chalcogenide electrodeposition processes are the most thoroughly studied ones, they are

described separately as are also the few earlier lead chalcogenide electrodeposition studies. Then the electroanalytical techniques, cyclic voltammetry and electrochemical quartz crystal microbalance, which were used in the present work, are presented. The last chapter in the background part deals with PbS, PbSe and PbTe thin films, their properties, preparation and applications. After the experimental details, the results achieved are summarized and discussed.

2. Background

2.1. Electrodeposition

Electrodeposition is an electrochemical liquid phase thin film or powder preparation method where the reactions, either reduction or oxidation, are accomplished using an external current source. The deposition is carried out in an electrochemical cell consisting of a reaction vessel and two or three electrodes. In the two electrode cell the reactions are controlled by the current applied between a working electrode (substrate) and a counter electrode. In the three electrode cell a reference electrode is used to control or measure the potential of the working electrode, and depositions are carried out by controlling either current or potential and the corresponding potential or current, respectively, may be measured.

The first invention concerning the electrochemical preparation techniques was Volta's discovery of the chemical way to produce electricity in 1799 which led to wide interest of electrolysis. At the first stage, the electrodeposition was mainly focussed on the deposition of copper from its simple salts, but deposition products were probably powdery rather than smooth, dense films. Forty years later the importance of a complexing agent, cyanide, was introduced, which allowed also the deposition of other metals like gold, lead and zinc. The use of cyanides in plating paths also made the deposition of thin and dense films possible. [1]

Electrodeposition of metals is commonly carried out galvanostatically, i.e. with constant current applied between the electrodes. No reference electrode is needed which makes the galvanostatic system very practical but it can be used only if the chemical composition of the deposit does not have to be controlled by the applied potential. The potentiostatic electrodeposition, i.e. deposition at controlled, constant potential is the most often used mode in a compound deposition where the stoichiometry of the product needs to be strictly controlled.

In addition to the constant potential and current techniques, the deposition may also be carried out with the pulse mode, where the potential or current is pulsed between two different values or between a constant value and an open circuit.

With the pulsed deposition better adhesion or morphology may be achieved, for example.

Compound electrodeposition can be carried out either cathodically or anodically, i.e. the working electrode is a cathode or an anode, respectively, and the deposition reactions are accordingly reductions and oxidations. In the anodic system the substrate, anode, is made of a metal which is a constituent of the product compound, for example lead in the deposition of PbS. In cathodic deposition, the choice of the substrate material is not limited, basically any conducting material may be used.

In addition to the one step deposition process presented above, compounds may be grown by depositing first elemental layers which are then suitably annealed. The annealing be carried out under various atmospheres, reactive or inert, depending if the composition of the product needs to be altered. The initially deposited layers may also consist of different compounds, for example $CuSe_x$ and $InSe_y$, if the final product is $CuInSe_2$. Electrodeposition is also possible from molten salts but that is excluded from this presentation.

The potential where a reduction reaction occurs can be estimated from the Nernst equation, which is (1) for the reaction (2):

$$E = E^\circ - \frac{RT}{zF} \ln\left(\frac{a(M)}{a(M^{z+})} \right)$$ (1)

$$M^{z+} (aq) + ze^- \leftrightarrows M (s)$$ (2)

where β is the reduction potential, E° is the standard potential for the reaction (2), R the gas constant, T the temperature, F the Faraday constant, z the number of electrons, and $a(M)$ and $a(M^{z+})$ are the activities of M and M^{z+}. Activities of the ions are usually approximated to be the same as the concentrations and the activity of a pure element is one. The calculated potential is valid only under the equilibrium conditions, which are hardly met in practice. The reduction needs a certain overvoltage, which is the irreversible excess potential required for a reaction to occur. The origin of the overpotential may be for example adsorption reactions, concentration profiles, diffusion rates, nucleation, or reaction rates.

Therefore it is more useful to measure the actual reduction potential under the experimental conditions, for example by cyclic voltammetry which is discussed in Chapter 2.2.

In order to achieve a suitable potential range for the deposition process, the precursors can be complexed which shifts their reduction potentials. When the metal ion M^{z+} is complexed with a ligand L^{p-}

$$M^{z+} + qL^{p-} \leftrightarrows ML_q^{z-pq} \tag{3}$$
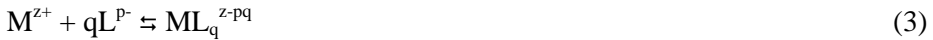
it's reduction potential is shifted according to the equation (4):

$$E = E^\circ_{M^{z+}} - \frac{RT}{zF}\ln\beta + \frac{RT}{zF}\ln\left(\frac{a(ML_q^{z-pq})}{a(L^{p-})^q\,a(M)}\right) \tag{4}$$

where β is the stability constant of the complex. The use of the complexing agent may also be necessary to prevent unwanted precipitation in the precursor solution. Complexing agents are widely used in the industrial metal deposition processes as they stabilize the deposition solution, dissolve metals and improve the quality of the deposit.

A monolayer of an element may also deposit by under potential deposition (UPD), i.e. at the potential more positive than the equilibrium, bulk deposition potential. UPD occurs if the bonding energy between two different metal atoms is greater than the bonding energy between the deposit atoms and it is common for example for lead on noble metals.

2.1.1. Induced codeposition

Although the electrodeposition of alloys has been known for a long time [1], and also the electrodeposition of chalcogenide compounds has been studied earlier, for example the preparation of CdSe and Ag_2Se was reported in 1963 [2], the true development of the cathodic electrodeposition of semiconductor compounds started to accelerate as late as in 1978 when Kröger published thermodynamic calculations about the induced codeposition method [3] and the paper on the CdTe electrodeposition process [4]. According to Kröger, CdS, CdSe, and CdTe belong to the group where the deposition potential of a

compound is determined by the less noble component and it is more positive than the reduction potential of the less noble component itself. In that group, where PbS, PbSe, and PbTe also belong, the difference between the equilibrium potentials of the pure components ($\Delta E°$) is larger than the shift in a potential of either component (ΔE) caused by the compound formation. For example for PbSe, the maximum shift in the lead reduction potential, ΔE, may be calculated from (5)

$$\Delta E \;=\; -\frac{\Delta G°(\text{PbSe})}{zF} \;=\; -\frac{-101.7 \text{ kJ / mol}}{2 \text{ x } 96485 \text{ C / mol}} = 0.53 \text{V} \tag{5}$$

The difference in the equilibrium reduction potentials ($\Delta E°$)

$$\Delta E° = E° \, (Se^{4+}/Se) – E° \, (Pb^{2+}/Pb) = 0.778 \text{ V} – (\text{-}0.126 \text{ V}) = 0.904 \text{ V} \tag{6}$$

thus $\Delta E° > \Delta E$. In Eq. 6, values of $E°$ (vs. SHE) are adopted from [5] and $\Delta G°$ values from [6]. The formation of the compound instead of elemental layers is favoured by the energy gain in the reaction. A large excess of the metal precursor M^{2+} is needed in order to make the compound formation reaction more favourable than the reduction of chalcogen X^{4+} on top of itself. This should also ensure that the correct stoichiometry is obtained even if some concentration variation exists.

Since the reduction of the chalcogen induces the reduction of the metal to occur at a more positive potential than where it would reduce alone, the process is called as an induced codeposition. It is very close to the UPD process described earlier. A schematic picture of the induced codeposition of a compound MX, which may be for example PbSe, is shown in Fig. 1.

Three potential ranges E_1, E_2 and E_3 are distinguished in Fig. 1. At the potentials E_1 only the chalcogen X is deposited. At the more negative potentials, E_2, X induces the simultaneous reduction of the metal M^{2+} ion, and the compound MX is formed. Finally, at the most negative potentials, E_3, the reduction of M^{2+} to a metallic deposit becomes the dominating process.

c (M^{2+}) >> c (X^{4+})

1 (a) E_3 E_2 E_1 E (V)   I (A)

1 (b) E_1 $X^{4+} + 4e^- \rightarrow X$

1 (c) E_2 $M^{2+} + X^{4+} + 6e^- \rightarrow MX$

1 (d) E_3 $M^{2+} + 2e^- \rightarrow M$
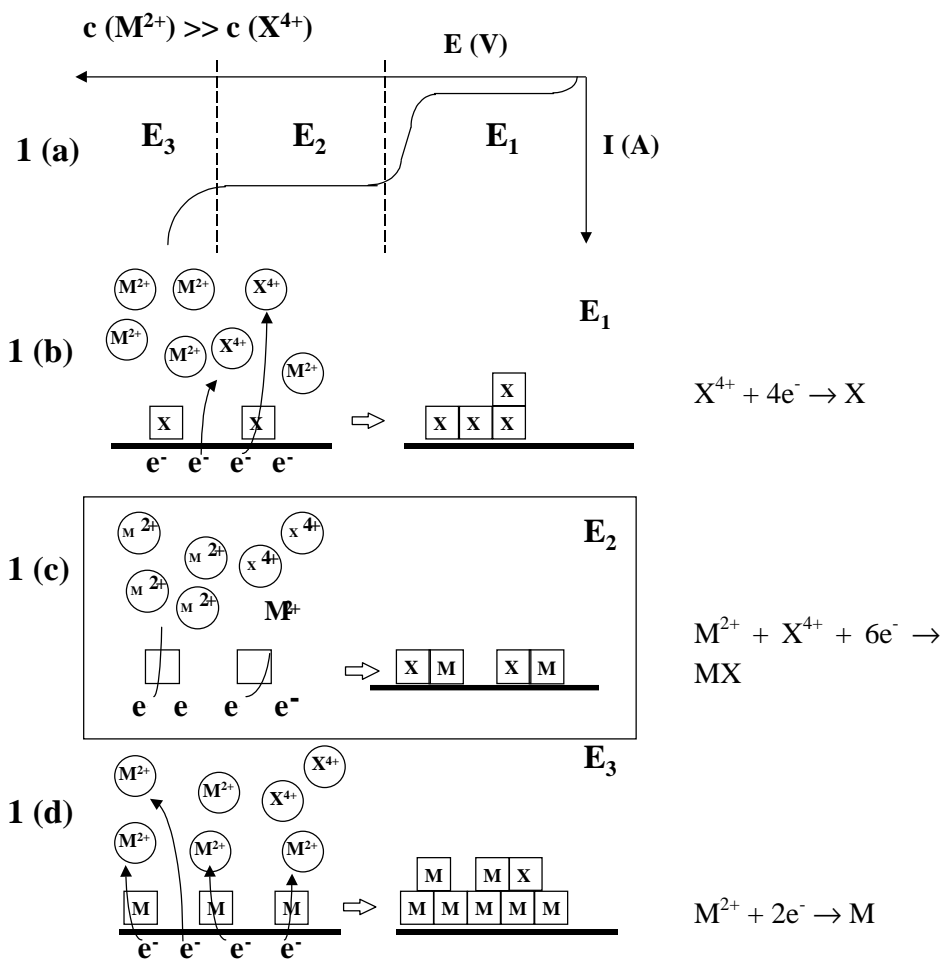
Figure 1. A schematic picture of the induced codeposition mechanism of the compound MX: 1(a) the current-voltage curve, and (b)–(d) the dominating deposition mechanisms at the different potential ranges. For simplicity, the aqueous species are denoted as M^{2+} and X^{4+} although they may be complexed or in the form of oxospecies.

2.1.2. Electrodeposition of binary chalcogenides

Among the binary chalcogenide electrodeposition processes, CdSe, CdTe and CdS are the most studied ones because of their very interesting application in solar cells, and therefore they are discussed here separately. Reference [7] reports a table which contains 21 references for CdS electrodeposition, 15 for CdSe and 31 for CdTe. In addition, there are many reviews available, for example [8]. The purpose of this presentation is not to be a complete review of the electrodeposition of cadmium chalcogenides, and the references cited here just give examples of the different aspects of the processes.

In addition to the binary compounds, the electrodeposition of ternary and even quaternary chalcogenides has been investigated widely. Solid solutions, such as $CdSe_{1-x}Te_x$, may be achieved moderately simply by having all the precursors in the solution at the same time provided that they are soluble, stable, and reducible under the same conditions. The situation is more complicated when the product is a compound with a strict stoichiometry, such as $CuInSe_2$. The electrodeposition of $CuInSe_2$, which also is a very promising solar cell material, has widely been studied [9 and references therein], but still the control of the stoichiometry is the most challenging task.

In the following chapters the electrodeposition of CdTe, CdSe and CdS thin films is discussed first. Then the electrodeposition of other binary chalcogenide films is reviewed. The electrochemical atomic layer epitaxy method and the electrodeposition of oxide films are mentioned very briefly, and finally few electrodeposition processes of PbSe, PbTe and PbS thin films are looked in more detail.

2.1.2.1. Electrodeposition of cadmium chalcogenides

The electrodeposition of CdTe is commonly carried out cathodically under constant potential in the aqueous H_2SO_4 solution using $CdSO_4$ and TeO_2 as precursors. In most studies Kröger's induced codeposition methodology [4] is used, i.e. the concentration of Cd^{2+} is much larger than that of Te^{4+}. The pH of the solution is moderately low, 1–2.5, due to the scarce solubility of TeO_2 between pH 2 and 7 [10]. The main problem in the process is that an excess of Te is very easily deposited, but it can be diminished using very strict control

over the deposition potential [11]. Earlier, alkaline solutions were not used because in some studies it was observed that the deposit formed at high pH is powdery and of a poor quality. [12] It was stated that the deposition of high quality CdTe is not possible because, according to Pourbaix diagram, elemental Te is not stable in the alkaline solution. [12] Recently, however, Murase et al. [13–15] have deposited nearly stoichiometric, good quality CdTe films also from the alkaline solution, at pH 10.7.

In addition to pH and concentrations, the substrate has also been found to be very critical for the composition of the product. The films deposited on CdS and GaAs were stoichiometric, but those deposited on graphite were Te rich and the deposition of a good quality film on a Si surface was very difficult. [16] In addition, a reduction of a SnO_2 substrate in a $NaClO_4$ solution prior to the CdTe deposition has been found to improve the stoichiometry. [17]

CdTe films which are electrodeposited at the room temperature are usually amorphous, but those deposited at higher temperatures are polycrystalline with the cubic structure. However, the electrodeposition of monocrystalline CdTe films has been achieved using both polycrystalline SnO_2 [18] and monocrystalline InP [19] as substrates. In the latter case the epitaxial growth was verified.

CdSe is ordinarily deposited analogously to CdTe in an acidic solution using SeO_2 as precursor. However, in order to avoid excess Se in the films, CdSe has been deposited also in alkaline solution using *in situ* prepared $SeSO_3^{2-}$ where selenium has an oxidation state lower than 4+. [20, 21] In addition, for the same reason, KCN has been used to complex Se and Te in the CdSe and CdTe depositions in alkaline solutions [22]. Due to the instability of the Se^{2-} and Te^{2-} species the anodic processes are less studied with few exceptions [23, 24].

The CdSe and CdTe depositions are commonly carried out from uncomplexed solutions but complexing agents such as ethylenediaminetetraacetic acid (EDTA) [21], nitrilotriacetic acid (NTA) [20] and NH_3 [13–15] have also been used. The complexing is essential in the alkaline solutions where cadmium, and metals in general tend to precipitate as hydroxides.

Organic solvents, such as dimethylsulfoxide (DMSO) [18, 25], and ethylene glycol [26], have been used as well in order to be able to use chalcogen

precursors with oxidation state lower than 4+. In those cases the chalcogen is normally in the elemental form whereas the metal is as a cation, exception are the studies where CdTe and CdSe were deposited in propylene carbonate and diethylene glycol using tri(n-butyl)phosphine telluride [27] or selenide [28]. CdSe and $CdSe_xTe_{1-x}$ thin films have been deposited also from a solution containing both water and ethylene glycol [26] with SeO_2 and TeO_2 as precursors at pH 2.2.

Commonly, the electrodeposition is carried out using a constant potential or current, but there are examples of the pulsed CdS [29, 30], CdTe [29, 31] and CdSe [32] or cycled CdSe [33] and CdTe [34] deposition systems. The pulsed deposition was found to improve adhesion [29]. In addition, the film structure was more compact and uniform [31] and the grain size was found to increase. [32] The improvement of the film structure has been proposed to be due to nucleation which occurs during the first pulse stage and the unwanted small nuclei disappear during the subsequent pause stage. The cyclic deposition mode was also found to improve the stoichiometry of CdSe. [33]

Electrodeposition of CdS, as well as other metal sulfides, differs from the conventional CdTe and CdSe processes where the oxidation state of tellurium and selenium precursors is 4+. An analogous sulfur precursor, SO_3^{2-}, is not used due to its instability. On the other hand, the most common sulfur precursor, $S_2O_3^{2-}$, is not stable either and decomposes in the acidic solution according to the reaction (7)

$$S_2O_3^{2-}(aq) \leftrightarrows S(coll.) + SO_3^{2-}(aq) \tag{7}$$

Therefore the electrodeposition of cadmium sulfide films is predicted to occur via adsorption of colloidal sulfur and subsequent induced reduction of cadmium.

$$Cd^{2+}(aq) + S(ads.) + 2e^- \leftrightarrows CdS(s) \tag{8}$$

However, incorporation of colloidal sulfur into the films may cause nonstoichiometry and irreproducibility problems. In addition, the solution ageing during the deposition may become a problem. On the other hand, in the alkaline solutions deposition has not been successful probably because the reduction potentials of both $S_2O_3^{2-}$ and complexed Cd shift to such negative

values that hydrogen reduction becomes a competitive reaction for the film growth.

CdS films have also been deposited anodically from an alkaline solution. The disadvantage is that in the conventional anodic process a cadmium substrate is needed and in the most cases the film thickness limited and the quality of the film is poor. In order to avoid the stability problems, CdS has been deposited in organic solvents, such as DMSO [35], diethylene glycol [36] and propylene carbonate [37].

2.1.2.2 Electrodeposition of other metal chalcogenides

Table 1 represents an overview of the other electrodeposited binary chalcogenides, except lead and cadmium chalcogenides. Most of the deposition processes are very similar to the original CdTe process and not very many are carried out in organic solvents. Complexing agents have been used in some studies, EDTA in refs. [38–42] and acetate in ref. [43]. Both potential and current control have been used but in general more stoichiometric, adhesive and dense films have been produced potentiostatically. Especially the chemical composition is difficult to control in the galvanostatic mode. On the other hand, the film compositions have often been determined only by EDX, the accuracy of which may be only about 5 %, and by XRD which only detects crystalline phases of the film. Therefore it is very difficult to conclude the accurate stoichiometry of the films.

Though it was stated above that in the alkaline solutions the reduction potential of $S_2O_3^{2-}$ is too negative to be useful, an example of a dissimilar situation is the electrodeposition of Ag_2S. [38] Silver is the more noble component and even when complexed with EDTA its reduction potential remains close to zero. In that case silver induces the codeposition of sulfur. Another type of sulfide deposition involves an electrochemical conversion of the evaporated CdS films to Cu_xS. [44]

In the aqueous solutions the depositions are normally carried out at room temperature, but higher temperature experiments have also been carried out. [44–48] In the organic solutions higher temperatures, 100–165 °C, are used without an interference of the evaporation of the solvent. The higher deposition

temperature in general increases the crystallinity of the films. In addition, it may be used to increase the solubility of the precursors, for example TeO_2. The high temperature also increases the deposition rate by enhancing the diffusion. Another way to enhance the deposition rate is stirring, accomplished usually with a simple magnetic stirrer, which has also been found to have positive effects on the film quality. [41, 49–54]

In comparison with the other metal chalcogenides, the electrodeposition of tin chalcogenides is more difficult due to the very poor stability of Sn^{2+} and Sn^{4+} in the aqueous solution. In addition, Sn^{2+} tends to reduce Se^{4+} to Se^{0} in the deposition solution. EDTA has been used to stabilize the solution but the problem has not been totally avoided, for example in ref. [40] it is mentioned that the solution was stirred to homogenise the viscous, gelatinous mass.

Electrodeposition of chalcogenides is usually carried out from a single solution where separate precursors for metal and chalcogen are diluted. However, FeS_2 [55] and In_2S_3 [56] films have been deposited sequentially using different solutions for sulfur and iron or indium precursors. MoS_2 films has been deposited by reducing a single compound, MoS_4^{2-}, which was synthesised in the solution prior the film growth. [57–59]

Table 1. An overview of the electrodeposited binary chalcogenide compounds, except lead and cadmium chalcogenides. Only chalcogen precursors are listed since in general the metal precursor is a metal cation in the solution and its counterion appears to have no effect.

[a] ac = acidic, alk = alkaline, org = organic deposition solution, pH is given if reported, organic solvents: DEG = diethylene glycol, PG = propylene glycol, EG = ethylene glycol, FA = formaldehyde, DMF = dimethyl formamide, [b] a = anodic, c = cathodic process, [c] p = potentiostatic, g = galvanostatic deposition.

* Deposition of metal and chalcogen was carried out sequentially using different deposition solutions.

Material	ac/alk/org[a]	a/c[b]	p/g[c]	Chalcogen precursor	Excess species or phase mixture	Ref.
Sulfides						
Ag_2S	pH 2	c	p	$Na_2S_2O_3$		38
Ag_2S	pH 10	c	p	$Na_2S_2O_3$		38
As_2S_3	pH 2	c	p, g	$Na_2S_2O_3$	S excess	42
Bi_2S_3	pH 2	c	p, g	$Na_2S_2O_3$	S excess	42
Bi_2S_3	org DEG	c	g	S		49
Bi_2S_3	alk	a	p, g	Na_2S		60
Bi_2S_3	alk	a	p	Na_2S		61
Cu_2S	alk	a	p	Na_2S		62
Cu_2S	alk	a	p, g	Na_2S		63
Cu_2S	alk	a	p	Na_2S		64
Cu-S	org PG	c	p	S	mixture	41
Cu-S	ac	c	g	–	mixture	44
Cu-S	pH 2.5	c	p	$Na_2S_2O_3$	mixture	65
FeS_2*	alk S ac Fe	a	p	Na_2S		55
Fe-S	pH 2.0–6.5	c	p	$Na_2S_2O_3$	S excess	66
In_2S_3*	alk S ac In	a	p	Na_2S		56
MoS_2	pH 8.0	c	p	$(NH_4)_2MoS_4$		57

Material	ac/alk/org[a]	a/c[b]	p/g[c]	Chalcogen precursor	Excess species or phase mixture	Ref.
MoS_2	org EG	c	p	$(NH_4)_2MoS_4$	S excess	58
MoS_2	org EG	c	g	$(NH_4)_2MoS_4$	Mo excess	59
Sb_2S_3	pH 2	c	p, g	$Na_2S_2O_3$	S excess	42
Sb_2S_3	pH 9.0	a	p, g	Na_2S		67
SnS	pH 1.5	c	p	$Na_2S_2O_3$	S excess	39
SnS	pH 1	c	p	$Na_2S_2O_3$		40
SnS	org various	c	g	S		50
SnS	org EG	c	p, g	S	Sn excess	51
SnS	pH 3–4	c	p	$Na_2S_2O_3$	Sn excess	68
Y-S	org FA	c	p	CH_3CSNH_2	mixture	43
ZnS	pH 2.5	c	p	$Na_2S_2O_3$		69
ZnS	pH 8–10	c	p	$Na_2S_2O_3$		70
Selenides						
Bi_2Se_3	ac	c		SeO_2		71
$Cu_{2-x}Se$	pH 2.7–3.1	c	p	SeO_2	Se excess	9
Cu-Se	pH 1.7–2.5	c	p	SeO_2	Se excess	72
Cu-Se	pH 1.4	c	p	SeO_2	Se excess	73
Cu-Se	pH 1.8	c	p	SeO_2	mixture	74
Cu-Se	pH 1.4	c	p	SeO_2	mixture	75
In_2Se_3	pH 3.35	c	p	SeO_2		76
In-Se	pH 1.5	c	p	SeO_2	Se excess	72
In-Se	pH 1.2	c	p	SeO_2	Se excess	73
In-Se	pH 1.5–1.7	c	p, g	SeO_2	g → Se excess	77
In-Se	pH 1.7	c	g	SeO_2		78
$MoSe_2$	pH 9.7	c	g	SeO_2	mixture	79
$MoSe_2$	pH 9.7	c	g	SeO_2	mixture	80

Material	ac/alk/org[a]	a/c[b]	p/g[c]	Chalcogen precursor	Excess species or phase mixture	Ref.
Sb_2Se_3	ac	c	p	SeO_2		81
Sb_2Se_3	pH 1	c	p	SeO_2	Se or Sb excess	82
SnSe	pH 3	c	p	SeO_3	Se excess	83
SnSe	org DMF	c	p	Se	Se excess	83
SnSe	pH 2.8	c	p	SeO_2		84
WSe_2	pH 9.2	c	g	SeO_2	mixture	54
YSe_2	org FA	c	p	SeO_2	mixture	43
ZnSe	pH 2.0–2.5	c	p	SeO_2	Se excess	47
ZnSe	ac	c	p	SeO_2		85
ZnSe	pH 2.0	c	p	SeO_2	Se excess	86
ZnSe	pH 2.5	c	p, g	SeO_2	Se excess	87
ZnSe	ac	c	g	SeO_2		88
ZnSe	ac	c	g	SeO_2		89
Tellurides						
Bi_2Te_3	pH 0	c	g	TeO_2	Te excess	90
Bi-Te	pH 0.9	c	p	TeO_2	mixture	91
Y-Te	org FA	c	p	TeO_2	mixture	43
ZnTe	pH 2.5–5.6	c	p	TeO_2	pH<4 Te excess	45
ZnTe	pH 2.5–5.6	c	p	TeO_2	Te excess	46
ZnTe	ac	c	p, g	TeO_2	Te excess	48
ZnTe	org EG	c	p	$TeCl_4$		52
ZnTe	org EG	c	p	$TeCl_4$		53
ZnTe	ac	c	g	Te-rod as an anode		92

ECALE (electrochemical atomic layer epitaxy) is a different approach to the electrodeposition of compounds. In ECALE the compound constituents are deposited from separate solutions alternately one at the time and the deposition potentials, solution concentrations, pH's etc. can be optimized separately. The deposition potentials are chosen so that the compound constituents deposit at the UPD range, which should ensure that a monolayer is deposited and thereby the deposition process is very strictly controlled. ECALE has been applied to deposit CdS, CdSe, CdTe, ZnS, ZnSe, ZnTe, HgSe, PbSe and GaAs thin films. [93]

Although oxygen belongs to the same group with S, Se and Te, electrodeposition of oxides is quite different from the other chalcogenides since oxygen atoms are always present already in the aqueous solvent, molecular oxygen readily dissolves in water from air, and the stable oxidation state of oxygen is 2-. Metal oxide films may be deposited cathodically at potentials more positive than the metals themselves, for example ZnO [94] and Cu_2O [95], with either NO_3^- or molecular oxygen as the oxygen precursor, or anodically, for example PbO_2 [96] and ZrO_2 [97]. In both cases the oxide film is usually formed via dehydration of metal hydroxide. An overview of the oxide electrodeposition may be found from the recent review article. [98]

2.1.2.3. Electrodeposition of lead chalcogenides

Strel'tsov et al. have investigated the cathodic electrodeposition of all lead chalcogenides, PbSe [99, 100], PbTe [99] and PbS [101]. PbSe and PbTe electrodeposition processes were examined in 0.1 M HNO_3 using platinum substrates. [99, 100] PbSe films deposited from solutions containing 0.05 M $Pb(NO_3)_2$ and 0.001 M SeO_2 at potentials -0.1,–0.26 and -0.4 V vs. saturated Ag/AgCl electrode were found to be selenium rich (55–57 at.% Se). PbTe films deposited from 0.05 M $Pb(NO_3)_2$ and 0.001 M TeO_2 solutions at -0.3 V were Te rich but the amount of the Te excess in the films was smaller (49 at.% Pb – 51 at.% Te) than the amount of the Se excess in PbSe. The PbSe and PbTe films were crystalline with randomly oriented cubic structure as measured by XRD. Lead and cadmium sulfide multilayer films were electrodeposited by a pulsed potential method in an organic DMSO solution using elemental sulfur and lead and cadmium salts as precursors but the properties of the individual layers were not analysed. [101]

The electrodeposition of PbSe has also been studied in a solution containing EDTA as a complexing agent for Pb^{2+} [102]. Titanium and graphite were used as substrates and a rotating disc electrode was used in the electrochemical analysis. Stoichiometric films, as measured by EDX, were deposited from the solution where the concentration ratio of Se and Pb precursors was 0.5 but the actual concentrations and deposition potential were not reported. In addition, the authors concluded that Pb^{2+} catalyses the reduction of Se^{4+} which alone would reduce at a potential more negative than the reduction potential of Pb^{2+}[102] which is a quite unique statement and has not been confirmed in any other study.

PbS thin films have been electrodeposited by three methods: cathodically both in aqueous solutions [103–105] and in an organic solution [35], and anodically in an aqueous solution [106]. In addition, anodic PbS electrodeposition has been investigated by using a lead amalgam electrode [107] but the deposition was restricted to the first tens of monolayers. In the both anodic deposition studies [106, 107], only the deposition mechanism was studied but not the film properties. In two cathodic cases [103, 104], films were deposited in acidic solutions with low concentrations (0.001 M) of Pb^{2+} and $S_2O_3^{2-}$. In one study [103] titanium, aluminium and stainless steel substrates were used. The pH range where the deposition occurred was very narrow, from 2.7 to 2.9. In addition, the films were deposited only at one potential, -0.7 V vs. Ag/AgCl. According to XRD the films were (100) oriented on the stainless steel substrates. On the other hand, another phase, PbS_2, was found at pH 2.9 on the Al and Ti substrates, probably due to S_2^{2-} ions in the solution. In another cathodic study [104] the films were deposited at -0.6 V vs. Ag/AgCl and they were found to be stoichiometric. In the third cathodic deposition study [105], PbS was deposited from a solution containing 0.1 M Pb^{2+} with an excess of $S_2O_3^{2-}$, the latter serving as a complexing agent as well as the sulfur source. The substrate was (100) single crystal gold and the PbS deposit was epitaxial.

Besides thin films, lead chalcogenide powders have been synthesised electrochemically. For example, PbTe powder was made using Te anode and Pb cathode at pH 4.5 [108].

2.2. Cyclic voltammetry combined with electrochemical quartz crystal microbalance

Cyclic voltammetry is an electrochemical technique in which the potential applied to the working electrode of an electrochemical cell is scanned and the current due to the electrochemical reactions is measured. The potential scan is programmed to begin at an initial potential where no electrochemical reactions occur. The scan goes with a desired constant rate to the switching potential, then reverses direction and returns to the initial potential. The current is positive or negative if the reaction on the electrode is oxidation or reduction, respectively. Cyclic voltammetry can be used to analyse the electrochemical behaviour of species diffusing to the electrode, interfacial phenomena at the electrode surface, and the bulk properties of materials in or on the electrodes. Cyclic voltammetry is only semiquantitative, but very useful technique for finding suitable potential ranges for electrodeposition processes.

In the quartz crystal microbalance (QCM) method, the resonant frequency of a quartz crystal is monitored. The piezoelectric quartz crystal is forced to vibrate by introducing an alternating voltage between metal electrodes evaporated on both sides of the crystal (Fig. 2). That is called a converse piezoelectric effect and it is the basis of the QCM method. As the resonance frequency is dependent on the mass of the crystal, including also deposit layers on its surfaces, QCM offers an accurate way to measure deposit masses.
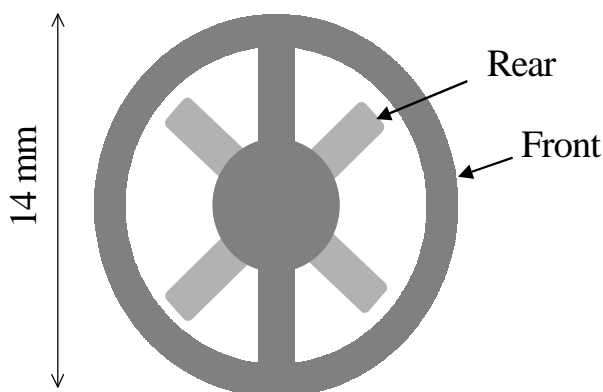
Figure 2. A schematic picture of the quartz crystal used in the QCM system. The dark areas represent metal electrodes evaporated on the both sides of the translucent crystal. The metal patterns may vary.

Changes in the resonance frequency of the crystal correspond directly to the mass changes of the crystal according to the well known Sauerbrey equation:

$$\Delta f = -\left(\frac{2f_0^2}{A\sqrt{\mu\rho}}\right)\Delta m = -K\Delta m \qquad (9)$$

where f_0 is the resonant frequency of the quartz crystal, A is the piezoelectrically active area, μ is the shear modulus of the quartz, and ρ it's density. The negative sign implies that the resonant frequency falls as deposition takes place. Quartz crystal microbalance is a convenient, very accurate technique for measuring film thicknesses and deposition rates *in situ* and it is routinely used in physical vapour deposition processes.

The theoretical sensitivity of a 5 MHz crystal, calculated from Eq. (9), is 17.7 ng Hz^{-1} cm^{-2}. For example, 1 Hz frequency change on the 1 cm^2 crystal during the deposition of Pb corresponds to a film thickness of 0.16 Å, which is well below the thickness of one monolayer. Factors affecting the sensitivity of QCM include roughness of the crystal and the deposit, size of the active area on the crystal surface, and the resonant frequency. Therefore it is convenient to calibrate the crystal under the experimental conditions. In addition, the vibration frequency should not decrease over 5% from the original value in order to maintain the reliability.

During the last fifteen years, the quartz crystal microbalance technique has been introduced into electrochemistry and many good review articles about the subject have been written since that. [109, 110] In an electrochemical cell, QCM may be combined with cyclic voltammetry measurement. The quartz crystal serves as a working electrode which allows simultaneous measurement of the mass and the current. The system is called as an electrochemical quartz crystal microbalance (EQCM). The quantification of the results is obtained by combining the Sauerbrey equation (9) with the Faraday law (10):

$$Q = znF \qquad (10)$$

A detailed description of the mathematical treatment of the measured data is presented in papers IV and V, and is not discussed here.

In the most simple situation EQCM is used to measure the thickness of the film, provided that the film composition and density are known. However, as EQCM is a very accurate technique, it has been used also in many other kinds of studies, for example to monitor the formation of monolayers of oxides and halides on Au, UPD of metals, adsorption and desorption of surfactant molecules, electrodeposition and corrosion processes and monolayer self-assembly. [109, 110] EQCM is especially useful in the analysis of the quite complicated electrochemistry of chalcogens. Due to their different solubilities, the various oxidation states of chalcogens may be distinguished easily from the mass variations. Figure 3 shows an example of the simultaneous cyclic voltammetry and EQCM measurement in a solution containing TeO_3^{2-}. As it seen, Te(IV) is soluble (mass does not change), Te(0) is insoluble (mass increases) and Te(-II) is soluble (mass decreases) under the present experimental conditions.

3 (a)
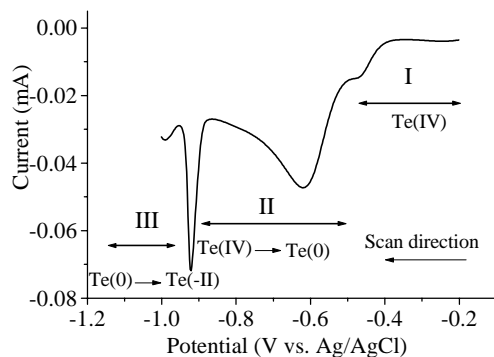
3 (b)
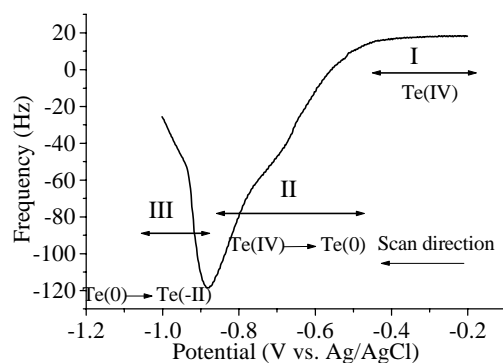
Figure 3. Cyclic voltammogram (a) and corresponding QCM curve (b) measured in a solution containing 0.001 M TeO$_3^{2-}$. For simplicity, TeO$_3^{2-}$ and HTe$^-$ are presented as Te(IV) and Te(-II).

Chalcogen and chalcogenide systems studies by EQCM include CdSe [111, 112], CuSe$_x$ [113, 114], CuInSe$_2$ [115], Te [116], CdTe [117, 118], In$_2$S$_3$ [56], FeS$_2$ [55] and Cu$_2$S [62]. In those studies EQCM has been used to analyse both the electrodeposition mechanisms [62, 113–116, 118] and the composition of the deposition products [111, 117], as well as to monitor that deposition occurs at the chosen potential [55, 56].

2.3. Lead chalcogenides

2.3.1. Properties

PbS, PbSe and PbTe are narrow band gap semiconductors. Their crystal structure is face-centred cubic, the coordination number in the structure is six, and the bond between Pb and S, Se or Te is considered to be mostly ionic. [119] The minimum energy gap E_g between the conduction band and the valence band is direct and the values for E_g are listed in Table 2 at different temperatures. The band gaps can be tailored by making solid solutions, such as $PbSe_{1-x}Te_x$ or $Pb_{1-x}Sn_xSe$. Table 2 contains also some other material characteristics of PbS, PbSe and PbTe.

Table 2. Band gaps, densities and static dielectric constants of PbS, PbSe and PbTe.

	PbS	PbSe	PbTe	Ref.
E_g at 77 K (eV)	0.307	0.176	0.217	119
E_g at 300 K (eV)	0.41	0.27	0.31	119
E_g at 373 K (eV)	0.44	0.31	0.34	119
ρ (g cm^{-3})	7.61	8.15	8.16	6
Static dielectric constant	161	280	360	6

Lead sulfide, selenide and telluride have many special characteristics in comparison with other semiconductors: [119]

1. The band gaps are smaller at lower temperatures, i.e. the temperature coefficients of E_g are positive while they are negative for all other elemental or compound semiconductors.

2. The lattice structure may be very unstoichiometric. The vacancies and interstitials control the conductivity type, an excess of Pb causes n-type conductivity and excess of chalcogenide causes p-type conductivity.

3. The band gap of PbSe is smaller than the band gap of PbTe, although commonly the band gap in the metal chalcogenide semiconductors diminishes as the atomic number of the chalcogenide increases.

4. The static dielectric constants of lead chalcogenides are much larger than those of the other semiconductors, for example for Si, GaAs, and InAs they are 11.8, 13.2 and 14.6, respectively. [6]

2.3.2. Film deposition

Lead chalcogenide thin films have been prepared by several gas phase techniques: evaporation [120, 121], molecular beam epitaxy (MBE) [122–125], hot wall epitaxy (HWE)[122–124, 126] and sputtering [127]. In addition, PbS films have been deposited by chemical vapour deposition (CVD) [128, 129] and atomic layer epitaxy (ALE) [130, 131]. Liquid phase techniques chemical bath deposition (CBD) [132–156] and successive ionic layer adsorption and reaction (SILAR) [157–159] have been applied to the deposition of both PbS and PbSe thin films. In addition, liquid phase epitaxy (LPE) has been used to deposit epitaxial lead chalcogenide thin film structures. [160] Electrodeposition, which was presented in the chapter 2.1.2.3. has been applied to the deposit all lead chalcogenides, as is also verified by the present study.

CBD is the oldest and the most studied PbSe and PbS thin film deposition method. It was used to deposit PbS already in 1910. [133] The PbSe and PbS films used in the commercial IR detectors are made by CBD. The basis of CBD is a precipitation reaction between a slowly-produced anion (S^{2-}, Se^{2-} or Te^{2-}) and a complexed metal cation. The commonly used precursors are lead salts, $Pb(CH_3COO)_2$ or $Pb(NO_3)_2$, and thiourea $((NH_2)_2CS)$ [133–151] or thioacetamide (CH_3CSNH_2) [152] for PbS, and selenourea $((NH_2)_2CSe)$ [153], its methyl derivative [154] or sodium selenosulfate (Na_2SeSO_3) [153, 155, 156] for PbSe, all in alkaline solutions. Lead may be complexed with citrate [154], ammonia [155], triethanolnamine [148, 149] or by selenosulfate itself [156]. Most often, however, the deposition is carried out in highly alkaline solution where OH^- acts as the complexing agent for Pb^{2+}. [134–147] CBD of PbTe has not been studied much which is probably due to the very high instability of telluride precursors, such as tellurourea, in the solution. However, PbTe has been deposited chemically from the solution containing Te^{4+} which was reduced by adding hydrazine (N_2H_4). [161]

In CBD the film is formed when the product of the concentrations of the free ions is larger than the solubility product of the compound. Thus, CBD demands very strict control over the reaction temperature, pH, and the precursor concentrations. In addition, the thickness of the film is limited, the terminal thickness is usually 300–500 nm. Therefore in order to get a film with a sufficient thickness, about 1 µm in IR detectors, for example, several successive depositions must be done. In comparison with gas phase techniques, the benefit of CBD is that it is a low cost and temperature method, and the substrate may temperature sensitive with various shapes.

2.3.3. Applications

Owing to their suitable band gaps, PbSe and PbS thin films are widely used in IR detectors. PbS is suitable for the detection of the radiation between wavelengths 1 and 3 µm and PbSe between 3 and 7 µm. Both detectors can operate at any temperature between 77 and 300 K. [132] On the other hand, Nair et al. have discussed the possibility to use very thin (20–60 nm) chemically deposited PbS films as solar control coatings. [148, 149] In addition, PbTe has been investigated for thermal applications, such as thermophotovoltaic cells. [120, 162, 163] In addition, as a trend of this time, nanocrystals and quantum size effects of lead chalcogenides deposited, for example, chemically from solution [164], gas phase [165] and aerosol [166] have been reported. In addition, quantum wells as well as other structures, grown by MBE and HWE have been studied for mid-infrared laser applications. [160, 167] However, since IR detectors are the most important application of lead chalcogenide thin films, they are discussed in more detail in the next few paragraphs.

Infrared radiation may be detected by using either thermal detectors or photodetectors. In the former, the IR radiation rises the temperature of the detector, which causes changes in the resistance (bolometer) or generates voltage (thermopile and pyroelectric detector). In the photodetectors, to which PbSe and PbS detectors also belong, the radiation produces electrons and holes in the detector material. Historically, thermal detectors, thermopiles and bolometers, were the only IR detectors before World War II. [168]

The photodetectors may be either photoconductors or photovoltaics, where the IR radiation increases the current or the voltage in the device, respectively.

Important parameters of the IR photodetectors are sheet resistance ($R_\square$), time constant (τ), detectivity (D^*), and the wavelength or the wavelength range where the detector is sensitive (λ). Time constant, the unit of which is s, describes the speed of response to a pulse of radiation. Detectivity describes the IR detector signal to noise ratio normalized to a detector active area of 1 cm^2 and a noise equivalent bandwidth of 1 Hz, and its unit is cm Hz$^{1/2}$ W^{-1}. D^* is stated for a specific wavelength, a chopper frequency, and noise equivalent bandwidth, for example D^*(4 μm, 1000 Hz, 1 Hz). D^* may also be measured at the wavelength of maximum spectral responsivity and then the resulting parameter is denoted as D^*(peak). All the parameters are strictly dependent on the measurement temperature. In general, the detectivity and the resistivity are at maximum and the time constant at minimum at low temperatures because of a decrease of noise in cold.

2.3.3.1. Photoconductor detectors

The incident radiation decreases the resistivity of a photoconductive film by creating electronic transitions between the valence and conduction bands. In the polycrystalline lead chalcogenide films the conductivity increase is partially due to the increase in the number of the free carriers, electrons and holes, and partially to the decrease in the potential barrier at the grain boundaries, which increases the mobility of the carriers. [119, 169] The definite mechanism has remained difficult to assign due to the several simultaneous processes.

In the IR devices, photoconductive films are usually deposited on quartz or sapphire substrates. On the top of the film gold electrodes are deposited either by vacuum evaporation or electroless plating. [132] In addition to PbSe and PbS, HgCdTe and InSb are used as photoconductive materials in IR detectors. [170, 171]

In order to obtain high performance detectors, lead chalcogenide films need to be sensitized by oxidation. The oxidation may be carried out by using additives in the deposition bath, by post deposition heat treatment in the presence of oxygen, or by chemical oxidation of the film. The effect of the oxidant is to introduce sensitizing centres and additional states in to the band gap and thereby increase the lifetime of the photoexcited holes in the p-type material. [169] In

some PbSe films, the oxygen concentration has been stated to be as high as 64 at.% after the sensitization as measured by electron probe microanalysis. [132]

In the old literature, unfortunately, the additives are very seldom identified and are often referred only as "an oxidant". [169, 172] A more recent paper deals with the effects of H_2O_2 and $K_2S_2O_8$ both in the deposition bath and in the post deposition treatment. [150] It was found that both treatments increase the resistivity and sensitivity of PbS films. For example, the increase in $R_\square$ during the H_2O_2 post deposition treatment was from about 65 kΩ $\square^{-1}$ to 200–400 kΩ $\square^{-1}$. [150] Photosensitivity, which was defined as $(R_{\square dark} - R_{\square illuminated}) / R_{\square illuminated}$, was found to be ten times larger after the H_2O_2 treatment. In comparison, during the heat treatment at 75 °C for 8 hours in air, $R_\square$ of PbS films increased from about 100 kΩ $\square^{-1}$ to 700 kΩ $\square^{-1}$ and photosensitivity increased from 0.14 to 1.64. [151] In both cases the thickness of the films was 0.12–0.2 µm.

Although the resistivity usually increases during the oxidation, a different behaviour has also been observed, as in one study the resistivity of a PbSe film dropped from 90 MΩ cm to 30 Ω cm after an annealing for 24 h at 100 °C in air. [156] The cooling rate has been found to affect the resistivity as well, the faster the cooling was done, the higher the final resistivity was. [153] Ordinarily after the deposition PbS films are annealed between 80–120 °C and PbSe films at a higher temperatures around 400 °C. [132]

The lead chalcogenide films are very susceptible to the adsorbed oxygen and water. A sensitized PbS film may significantly degrade in air without an overcoating. [173] Possible overcoating materials are As_2S_3, CdTe, ZnSe, Al_2O_3, MgF_2, and SiO_2. [173] Vacuum deposited As_2S_3 has been found to have the best optical, thermal and mechanical properties, and it has even improved the detector performance. [173] The drawback of the As_2S_3 coating is the toxicity of arsenic and its precursors.

Overall, however, the electric properties, resistivity and in particular detectivity, of lead chalcogenide thin films are rather poorly reported although there are so many papers on the film growth of especially PbS and PbSe. The effects of annealing and oxidation treatments on detectivity are not reported accurately either. Examples of the parameters measured for the photoconductive devices deposited by various techniques are listed in Table 3. For comparison, properties of commercial uncooled PbS and PbSe photoconductive detectors are

presented in Table 4. It can be concluded that the detectivities of the commercial PbS films are at the same level as those prepared in the laboratory whereas the performance of the commercial PbSe detectors are relatively far from the best laboratory devices.

Table 3. Properties of photoconductive IR devices prepared by various techniques.^{a}(4.0µm,10kHz,1Hz), ^{b}(330Hz,1Hz), ^{c}(4.5µm,800Hz,1Hz)

Film	Technique	$R_{\square}$ (MΩ $\square^{-1}$)	D* (cm Hz$^{1/2}$ W^{-1})	τ (µs)	T (K)	Ref.
PbS	CBD	0.5–2	~10^{11}	~10	300	172
PbS	ALE	0.1–0.2	5×10^{6}	<0.3	RT	130
PbSe	CBD	18	>10^{10} [a]	<0.3	300	174
PbSe	evaporation	0.2–0.8	5×10^{8}–10^{9} [b]		300	121
PbTe	sputtering	0.02–2	>8×10^{10} [c]	few	77	127

Table 4. Properties of commercial uncooled PbS and PbSe detectors. [170] ^{a}(λ,200Hz,1Hz), ^{b} (λ,600Hz,1Hz), ^{c} (λ,650Hz,1Hz), ^{d} (λ,1 kHz,1Hz).

Company	Film	$R_{\square}$ (MΩ)	D* (cm Hz$^{1/2}$ W^{-1})	τ (µs)	λ (µm)
SensArray	PbS	3–10	1.5–2.0x10^{11} [a]	>400	1.0–3.0
Hamamatsu	PbS	0.1–1	1.0x10^{11} [b]		2.2
Cal Sensors	PbS	1.0	1.0x10^{11} [c]	200	2.4
N.E.P.	PbS	0.2–2.0	0.5–1.2x10^{11} [b]	<100	3.0
SensArray	PbSe	0.2–0.5	2x10^{9} [d]	<2	2.0–5.0
Hamamatsu	PbSe	0.3–1.5	1.0x10^{9} [b]		3.8
Cal Sensors	PbSe	0.75	1.0x10^{9} [d]	2	3.8
N.E.P.	PbSe	0.1–4	1.0–3.0x10^{9} [d]	1–3	4.5–5.0

Although the detectivities of the detectors are high, the problem with CBD grown PbS and PbSe devices is that the properties of the films may vary from one deposition to another. [175, 176] Thus, all the detectors need to be tested and calibrated separately [175], which is complicated especially in the case of array detectors.

2.3.3.2. Photovoltaic detectors

The photovoltaic detectors consist of a p-n junction of either the same material (homojunction) or two different materials (heterojunction). The incoming radiation creates electron-hole pairs, which are separated by the electric field in the junction, thereby causing a detectable voltage over the junction. The films in the photovoltaic devices are commonly single crystal and epitaxial, i.e. the lattice structure of the film is ordered upon the substrate. Materials used in commercial IR-photovoltaics are for example InAs, InSb, PtSi, and HgCdTe. [170, 171]

Zogg et al. [122–124] have widely studied lead chalcogenide IR photovoltaics. In their studies, the lead chalcogenides have been deposited epitaxially on a silicon substrate by the MBE and HWE techniques using CaF_2 and BaF_2 buffer layers between the Si substrate and the lead chalcogenide films. A homojunction is formed by depositing a Pb layer on the top of the lead chalcogenide which inverts the surface region of the p-type lead chalcogenide to the n-type, thus creating a graded p-n junction. Silicon as a substrate makes the integration of the readout circuits easy. The resulting D* for a PbTe homojunction is $2x10^9$ cm $Hz^{1/2}$ W^{-1} at room temperature and that for PbS $5x10^9$ cm $Hz^{1/2}$ W^{-1} at 277 K. In a report by another group, the epitaxial PbSe homojunction grown by MBE [125] had D* of $3x10^9$ cm $Hz^{1/2}$ W^{-1} at 300 K and $\lambda = 4$ µm. In comparison, the PbTe-Si epitaxial heterojunction grown by HWE gave a detectivity D* = $1.6x10^9$ cm $Hz^{1/2}$ W^{-1} at room temperature and $\lambda = 4.26$ µm. [126]

Though the photovoltaic diodes consist usually of epitaxial films grown by the gas phase techniques at high temperatures, CBD grown polycrystalline diodes have also been studied. They are listed in Table 5. The heterojunction is formed directly between the substrate and the PbS film. The table includes only those studies where the approach of employing the heterojunction is discussed and measured. The effect of annealing or other post deposition treatments have not

been studied except in Refs. [141,142,147] with the following results, annealing at 100–300 °C $R_\square$ increased from 1–2 kΩ $\square^{-1}$ to 10–20 kΩ $\square^{-1}$,[141] heat treatment in air increased the oxygen and decreased the sulfur concentration at the film surface [142] and a few hours at 150 °C in air increased the signal-to-noise ratio by one order of magnitude [147].

Table 5. Heterojunctions grown by CBD. [a] s = single crystal, epitaxial PbS film, p = polycrystalline film.

Junction	s/p[a]	Resistivity (Ω cm)	D* (cm Hz$^{1/2}$ W^{-1})	τ (µs)	λ (µm)	Ref.
Ge-PbS	s	1.7–45		10 (RT)	1–4	134
Si-PbS	p			several	1–3	135
CdS-PbS	s	16				136
GaAs-PbS	p				0.85, 2.25	137
Ge-PbS	p			100 (77 K)		138
CdS-PbS	s		1.5 x10^{10}	200	3.3	139
GaAs-PbS			2 x10^{9} (77 K)		0.9–3.2	140
Si-PbS	p	5 (300 K)			1–3	141
Si-PbS	p					142
Si-PbS	p		1 x10^{10} (200 K)	1000 (200 K)	3	144–147
Ge-PbS	s					143
InP-PbS	s					143

3. Experimental

3.1. Cyclic voltammetry, EQCM and film growth

Cyclic voltammetry measurements and film growth experiments were carried out using a Metrohm 626 Potentiostat. An Autolab PGSTAT20 potentiostat combined with an EQCM equipment (Institute of Physical Chemistry, Warsaw, Poland) [177] was used to EQCM measurements. All the studies were carried out using a three electrode cell, graphite rod or platinum foil served as a counter electrode and saturated calomel electrode (SCE) or 3 M Ag/AgCl as a reference electrode. SnO_2 coated glass, Cu foil, Au film on glass, Pb foil or a silicon wafer were used as substrates, i.e. working electrodes. In addition, in the EQCM experiments unpolished quartz crystal covered with Au served as the working electrode. SnO_2 and Cu substrates were cleaned ultrasonically in water and ethanol before the experiments, the other substrates were used as received.

Due to the poor adhesion of PbTe and PbS films to the SnO_2 coated glass substrate, these substrates were pretreated by reducing them at the potential -0.95 V vs. Ag/AgCl in 0.1 M H_2SO_4 solution for 30–60 seconds. The adhesion was significantly improved after this treatment. Similar method has been used earlier when Cu was deposited on SnO_2 [178] and the improvement was suggested to be due to a combination of tin oxide surface roughening caused by preferential etching, *in situ* cleaning, and the stronger bonding between metallic Sn and Cu than SnO_2 and Cu. In CdTe studies, on the other hand, SnO_2 substrates have been reduced in a $NaClO_4$ solution [17] and the proposed mechanism was the reduction of Sn followed by the formation of SnTe when the substrate was immersed into the deposition solution.

The experiments were carried out at room temperature. The solutions were deaerated with 95.5 % purity nitrogen prior the EQCM measurements.

The precursor concentrations were chosen so that in the induced codeposition processes (PbSe, PbTe) the concentration of the chalcogenide was much smaller than the concentration of lead. In the case of PbS, the concentrations were chosen so that the spontaneous precipitation of PbS was avoided. The solutions used for electrodepositions contained 0.1–0.01 M $Pb(CH_3COO)_2$ complexed with an excess of EDTA, and 0.001 M SeO_2, 0.001 M TeO_2 or 0.01–0.001 M Na_2S in deionised water. In the cyclic voltammetry studies the concentrations of

the precursors were varied. In the EQCM measurements also solutions containing either only 0.1 M Na(CH$_3$COO) or both 0.1 M Na(CH$_3$COO) and 0.1 M EDTA were used as an electrolyte.

EDTA was used to complex Pb^{2+} in order to avoid the spontaneous precipitation of insoluble PbSeO$_3$, Pb(OH)$_2$ or PbS during the deposition of PbSe, PbTe and PbS, respectively. The PbSe deposition was studied at pH 3.5, PbTe at pH 9, and PbS at pH 8.5 and 5. NaOH and HNO$_3$ or CH$_3$COOH were used to adjust the pH. These pH values were chosen so that the PbEDTA^{2-} complex and all the other precursors were soluble and stable in the solution.

In the cyclic voltammetry measurements without EQCM the voltage scan rate was 0.1 V/s and in the cyclic voltammetry measurements combined with EQCM it was 0.01 V/s in the PbSe and PbTe studies. In the PbS studies the scan rate was varied between 0.01–10 V/s. Sampling rate of the EQCM frequency counter was 10 Hz.

3.2. Film characterisation

A Zeiss DSM 926 scanning electron microscope (SEM) of the Electron Microscopy Unit, Institute of Biotechnology, University of Helsinki, was used for imaging surfaces and cross sections of the films. Before imaging the samples were coated with a thin platinum layer using JEOL JFC-1100 sputter device. The cross sectional imaging was done from samples tilted 45°.

Thicknesses of the films were determined by a Dektak II profilometer and a Link ISIS Energy dispersive X-ray spectrometer (EDX) which was installed to the SEM equipment. A GMR electron probe thin film microanalysis program [179] was used to analyse the EDX results.

Compositions of the PbSe and PbTe films were analysed by EDX and Rutherford backscattering spectrometry (RBS). Deuteron induced reactions and elastic recoil detection analysis (ERDA) were used to analyse oxygen and hydrogen contents in the PbSe and PbS films while time-of-flight (TOF) ERDA was used to estimate oxygen and hydrogen contents in the PbTe films. In addition, chemical compositions of the PbS films were also analysed by a CAMECA SX50 wavelength dispersive X-ray analyser (WDX) at the Microprobe Laboratory of the Geological Survey of Finland.

Ion beam measurements were carried out at the Accelerator Laboratory at the Department of Physics, University of Helsinki. RBS, ERDA and deuteron induced reaction measurements were done using $^4\text{He}^+$ and $^2\text{H}^+$ ions from a 2.4 MV Van de Graaf accelerator and TOF-ERDA measurements using 53 MeV $^{127}\text{I}^{10+}$ from a 5 MV tandem accelerator EPG-10-II.

A Philips MPD 1880 powder X-ray diffractometer (XRD) using CuK_α radiation was employed in characterising film crystallinity. The step width was 0.020° and the time per step 1 or 2 s except during the more exact analysis of the d-values where the step width was 0.010° and the time per step was 20 s.

3.3. Electrical characterisation

3.3.1. Sample preparation

Electric properties of two types of samples, photoconductors and photovoltaic diodes, were examined. The photoconductive samples consisted of a lead chalcogenide film on a glass substrate (Fig. 4 (a) and (b)). The photovoltaic samples consisted of a PbSe or PbS film deposited on a Au electrode upon which a Pb layer had been deposited to form the homojunction (Fig. 4 (c)).

(a)

(c)

(b)

$\square$ = PbX $\blacksquare$ = Pb   ▨ = Au   ▨ = epoxy $\square$ = Glass
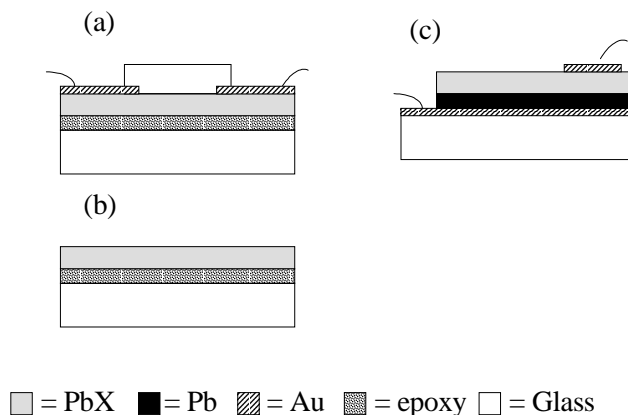
Figure 4. Schematic picture of photoconductive samples (a) and (b) and photovoltaic sample (c). Dimensions are not to scale.

Four point probe and hot point probe measurements as well as post deposition annealing experiments of the photoconductors were made with the samples shown in Fig. 4 (b) which were prepared by the following procedure. A lead chalcogenide film was deposited on a temporary substrate, which was a commercial Pb film on an acrylic foil (Goodfellow). The deposition potentials were -0.65 and -0.75 V vs. Ag/AgCl for PbSe and PbTe, respectively. PbS films were deposited between -0.45–-0.95 V in acidic solutions and between -0.60–-1.10 V vs. Ag/AgCl in alkaline solutions. After the deposition, the PbX film was glued to a glass substrate with an epoxy resin (Loctate). Then the acrylic film was removed with acetone. Finally, the Pb layer was dissolved electrochemically in a 0.1 M EDTA solution between the potentials -0.2 and -0.5 V vs. Ag/AgCl. The complete removal of Pb was verified by XRD measurements. The samples were annealed for various times in air at 85, 100 and 120 °C and some samples were dipped into a solution containing H_2O_2.

The photoconductor D* measurements were made with the samples depicted in Fig. 4 (a) which were prepared so that the Pb-acrylic foil was at first partially covered by gold which was electron beam evaporated through a mask. PbX films were then deposited on top of both gold and uncovered lead, and after that the films were glued and the lead substrate was removed as described above. The samples were annealed in air at 100 °C for 264 h and finally PbX was covered by a glass plate attached with the epoxy resin. D* values were measured at different temperatures between -60–+20 °C. The samples were capsuled and cooled by Pelter coolers.

The substrates in the photovoltaic samples (Fig. 4 (c)) consisted of gold films deposited by electrodeposition or electron beam evaporation on top of glass covered by Cr-Ni or Ni adhesion layer. A Pb layer (1 µm) was electrodeposited at -0.5 V vs. Ag/AgCl from a commercial Pb electroplating solution (Shlötter). A PbSe film (2–4 µm) was deposited on the Pb layer at -0.65 V and PbS (2–4 µm) between -0.45–-0.95 V, then the film was contacted by evaporated gold.

3.3.2. Measurement equipment

Resistance and resistivity values of the samples were measured by the four point probe method using Keithley 2400 SourceMeter and Alessi C4S Four Point Probe head. The conductivity types were determined by the hot point probe

method, where the hot end of a voltmeter (CEM DT-3900 Multimeter) was at the room temperature and the cold end (ground) was at the temperature of a liquid nitrogen. A positive voltage indicated n-type and negative voltage p-type conductivity. D* measurements were made at VTT Electronics or Rikola ltd in Oulu.

4. Results

In this chapter the main results of the author are summarised. More details will be found from the corresponding papers. In the following text all potentials are denoted versus 3 M Ag/AgCl (E^o = 0.207 V vs. H_2) reference electrode although some potentials are referred to saturated calomel electrode (SCE) (E^o = 0.244 V vs. H_2) in the original articles.

4.1. Film growth

PbSe and PbTe films were deposited for the first time by employing the induced codeposition method and using a complexing agent. In the induced codeposition system the large excess of metal precursor is used and the composition of a deposit is not affected by small variations in concentrations of precursors. On the other hand, the use of strong complexing agent such as EDTA enables the deposition over a wide potential range. In addition, the complexing agent allows higher pH in the deposition solution, as the formation of insoluble species, such as $PbSeO_3$, is avoided. PbSe was deposited in an acidic solution at pH 3.4 [I] and PbTe in an alkaline solution at pH 9 [II], because of the very low solubility of TeO_2 between pH values 2 and 7 [10]. In comparison, Strel'tsov et al. work [99, 100] was carried out in the 0.1 M HNO_3 solution from uncomplexed precursors.

PbS was deposited using a novel cyclic technique which involves an alternate cathodic and anodic reaction. [III] In contrast to conventional anodic process no lead substrate is needed. Since Na_2S is used as a sulfur source, the solution remains stable when made alkaline, as in the conventional cathodic process it is unstable. This method is based on cycling the substrate potential between two values with a symmetric triangle wave shape. A simplified reaction scheme is that at the negative, cathodic potentials (E_1), $PbEDTA^{2-}$ reduces to Pb:

$$PbEDTA^{2-}(aq) + H_2O + 2e^- \leftrightarrows Pb(s) + HEDTA^{3-}(aq) + OH^-(aq) \qquad (11)$$

and at the positive, anodic potentials (E_2), Pb reoxidises and reacts with sulfide ions according to the reaction (12) instead of complexing with EDTA or hydroxide ions.

$$Pb(s) + HS^-(aq) + OH^-(aq) \leftrightarrows PbS(s) + H_2O + 2e^- \qquad (12)$$
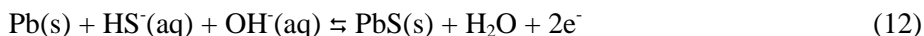
4.1.1. Deposition parameters and film compositions

4.1.1.1. PbSe [I] and PbTe [II]

The compositions of the electrodeposited PbSe and PbTe films measured by EDX are shown in Fig. 5. In all cases a rather wide potential range was found where the film composition was constant. RBS analysis showed that in that potential range the PbSe films were stoichiometric but PbTe films contained an excess of Te, the Pb:Te ratio was 45:55 at.%. At more positive potentials in the 0.01 or 0.05 M PbEDTA^{2-} solution the films were chalcogen-rich but in the 0.1 M PbEDTA^{2-} solution the deposition became so sluggish, that those, the most probably chalcogen-rich films, were not analysed at all. The films contained oxygen and hydrogen as impurities. The concentrations in the PbSe films were 8–12 at.% oxygen and 10–14 at.% hydrogen as analysed by deuteron induced reactions and ERDA, respectively. The origin of the impurities was obviously the aqueous deposition solution. Annealing under nitrogen at 200 °C for 1 h removed only ca. 20 % of hydrogen, thereby indicating that water was strongly bound to the films. The oxygen and hydrogen concentrations of PbTe films were analysed only semiquantitatively by TOF-ERDA, due to the difficulties arising from the large molar mass of Pb and Te and a rough film surface, and they were found to be rather similar than in the PbSe films.

5 (a)
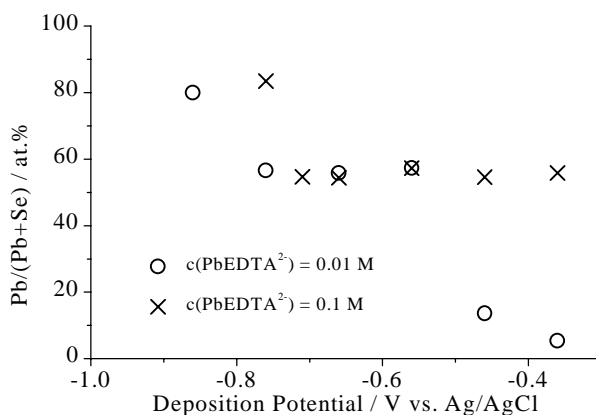
5(b)
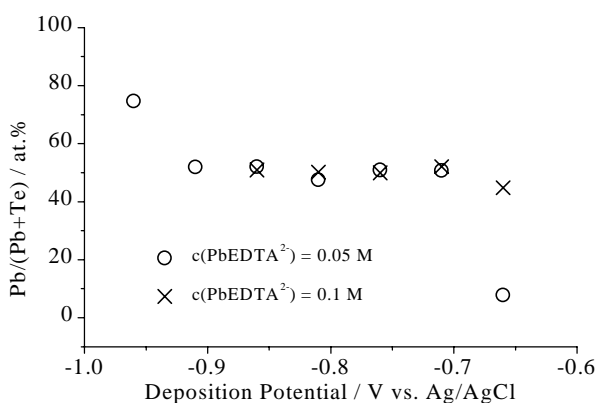
Figure 5. Composition of PbSe (a) [I] and PbTe (b) [II] films deposited at different potentials.

In comparison with the other metal-selenide electrodeposition processes, where the films are usually Se-rich (Table 1), in the present case the PbSe films were stoichiometric. A possible reason for that is the pH of the solution which in our case was higher than in the previous studies. At lower pH the reduction of Se continues to H_2Se at more positive potentials. H_2Se reacts with $HSeO_3^{2-}$ by eq. (13) and thereby increases the amount of Se in the films.

$$2H_2Se(aq) + H^+ + HSeO_3^-(aq) \leftrightharpoons 3Se^0(s) + 3H_2O \tag{13}$$
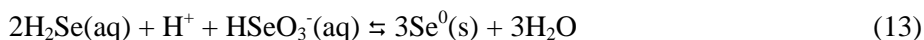
It has been claimed that CdTe can not be electrodeposited in alkaline solutions because of the instability of Te resulting in powdery films of poor quality. In our study, however, the films were shiny and dense if the SnO_2 substrate was reduced, i.e. the adhesion was improved. It is thus possible that the quality of CdTe films could also be improved by a similar adhesion enhancement procedure.

In the both cases of PbSe and PbTe, the current density remained constant, about -0.15 mA/cm^2, during the deposition, at the potential range where the constant composition was achieved. At more positive potentials it was lower, and at more negative potentials it started to increase because of the deposition of metallic lead. The growth rate of the films was about 0.25 µm per hour.

Some PbSe growth experiments were carried out using Si substrates. Before the deposition the substrates were dipped into a dilute HF solution to remove the nonconductive SiO_2 layer. However, the resulting films were nonadhesive and powdery which is probably due to a reformation of the native SiO_2 layer.

4.1.1.2. PbS [III,VI]

PbS films were deposited using fast potential cycling, 10 V/s at pH 8.5. Also lower cycling rates, 0.1 and 1 V/s, were examined but the resulting films were powdery and nonadhesive on the SnO_2 substrate. [III] The compositions and thicknesses of the PbS films deposited by cycling for 30 minutes using different end potentials, E_1 and E_2, are represented in Fig. 6. When E_1 was varied, E_2 was kept constant, -0.16 V, and when E_2 was varied E_1 was -1.36 V. Thicknesses of the films varied when the potentials were changed. Thickness of the films increased as E_1 was made more negative, i.e. more lead was deposited during the negative scan. On the other hand, if E_2 was more positive than -0.01 V PbS was dissolved by oxidation and if E_2 was more negative than -0.21 V deposition of PbS suppressed because during the short cycle not enough HS$^-$ diffused to the surface.

6 (a)
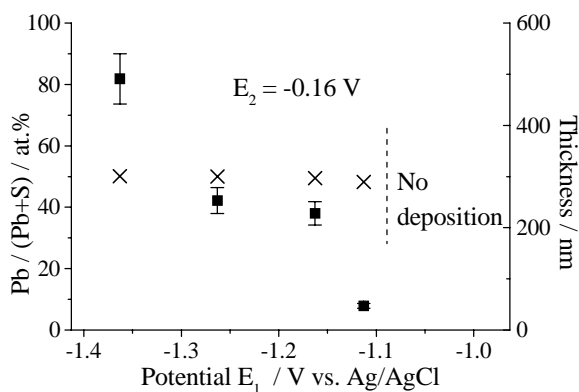
6 (b)
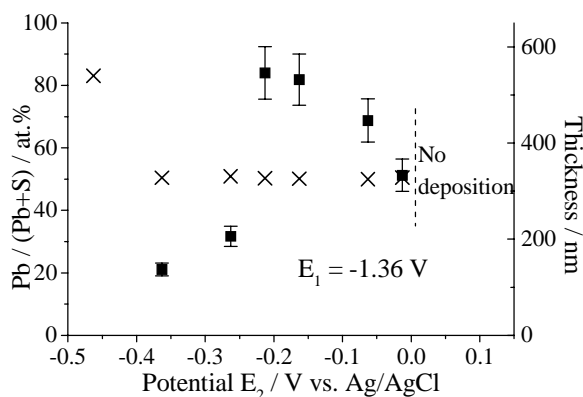
Figure 6. The compositions (cross) and thicknesses (square) of the PbS films deposited at pH 8.5 by cycling for 30 minutes using different end potentials, E_1 (a) and E_2 (b).

PbS thin films were deposited with the fast cycling rate also at pH 5 where H_2S oxidises to form colloidal sulfur. [III] It was found that the deposition potentials E_1 and E_2 did not affect the film composition if E_1 was more positive than -1.11 V and E_2 more positive than -0.66 V. In fact, films were deposited also at constant potentials between -0.51–-0.76 V.

The growth rates at the different pH's are compared in Fig. 7. In contrast to the alkaline solution, the deposition rate from the acidic solution diminishes as a function of the time, possibly because of the aging of the solution.
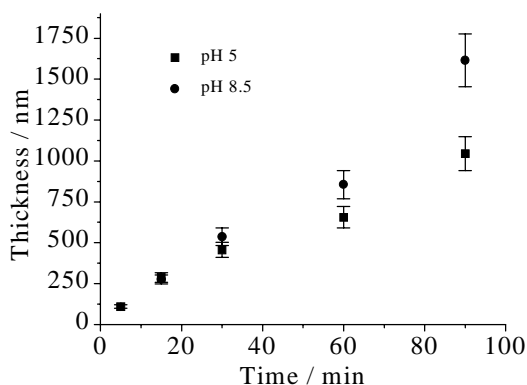
Figure 7. Film thicknesses vs. deposition time at pH 5 with potential cycling being carried out between -0.36 and -0.91 V and at pH 8.5 between -0.16 and -1.36.

Some PbS films were also deposited at pH 8.5 on the Au coated glass substrate using two slow scanning rates, 0.1 and 0.01 V/s. [VI] In contrast to the films deposited on the SnO_2 substrates [III] these films were bright and adhesive. The composition of the films are represented in the Table 6.

Table 6. Pb / (Pb + S) ratio measured by WDX for the films deposited on Au by cycling between the cathodic (E_1) and anodic (E_2) end potentials. For the last four potential pairs the composition of the films was not affected by the cycling rate.

E_1 V vs. Ag/AgCl	E_2 V vs. Ag/AgCl	Pb / (Pb+S) at.%	Scan rate V/s
-1.2	-0.5	82.3	0.1
-1.2	-0.5	92.7	0.01
-1.2	-0.4	77.8	0.1
-1.2	-0.4	94.0	0.01
-1.2	-0.3	52.9	0.1
-1.2	-0.2	52.5	0.1
-1.1	-0.2	50.9	0.1
-1.0	-0.2	50.8	0.1

Like the PbSe and PbTe films, also the PbS films contained hydrogen and oxygen as impurities but their concentrations were much smaller, only 1.7–2.0 and 1.3–1.9 at.%, respectively, as measured by ERDA and deuteron induced reactions. The fact that the PbS films contained less impurities, oxygen and hydrogen, than the PbSe and PbTe films is probably due to the large crystallites of PbS, since the impurities most likely lie in the grain boundaries and there are less grain boundaries in the more crystalline material. The impurity contents of the electrodeposited PbSe, PbTe and PbS films have not been studied by the other groups and therefore comparisons can not be made.

4.1.2. Morphology and crystalline structure

All the stoichiometric lead chalcogenide films were gray and mirror-like in appearance. At negative potentials the large excess of lead gave the films light gray colour. On the other hand, the excess of selenium gave red and tellurium black colour to the films. From SEM images it was seen that PbSe [I] and PbTe [II] were rather similar, though the PbTe films were somewhat rougher, but PbS differed having large, well defined cubic crystallites [III].

According to XRD, all the films were polycrystalline, cubic and randomly oriented. [I–III,VI] In the PbSe films XRD also indicated changes in the interplanar distances (d-values) as a function of deposition potential. [I]

4.2. Cyclic voltammetry and EQCM

The electrochemical behaviour of the precursors and the possible growth potential ranges were analysed in a preliminary manner by cyclic voltammetry (I,II) but since the mechanistic studies were carried out in more detail by the combined cyclic voltammetry and EQCM studies, only those results are summarised in this chapter. For figures see the original articles.

4.2.1. PbSe [IV]

At first, the electrochemical behaviour of selenium and lead precursors were measured separately at pH 3.5. EQCM studies on Au showed that before the Se bulk deposition its under potential deposition (UPD) occurs between the potentials -0.2–-0.4 V. The bulk deposition of Se by reaction (14) occurs

between -0.4–-0.7 V before the formation of HSe⁻ and reduction of hydrogen become dominating.

$$HSeO_3^- (aq) + 5H^+ (aq) + 4e^- \leftrightarrows Se(s) + 3H_2O \tag{14}$$
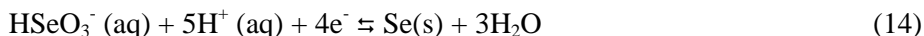
H_2Se formation on the previously deposited Se film was observed to begin at -0.45 V (reaction (15))

$$Se(s) + 2H^+(aq) + 2e^- \leftrightarrows H_2Se(aq) \tag{15}$$

$PbEDTA^{2-}$ was found to reduce at -0.95 V on the Au electrode (reaction (16)).

$$PbEDTA^{2-}(aq) + 2H^+(aq) + 2e^- \leftrightarrows Pb(s) + H_2EDTA^{2-}(aq) \tag{16}$$
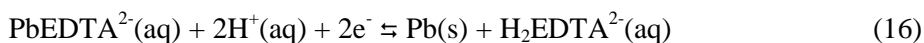
The oxidation of Pb was complicated since three oxidation waves were observed. It is proposed that they are due to the slow complexation of Pb^{2+} with EDTA and adsorption and desorption of $PbEDTA^{2-}$.

In a solution containing both lead and selenium precursors the deposition of PbSe was found to occur by the six electron reduction reaction (17) between -0.3–-0.7 V.

$$PbEDTA^{2-}(aq) + HSeO_3^-(aq) + 7H^+(aq) + 6e^- \leftrightarrows PbSe(s) + H_2EDTA^{2-}(aq) + 3H_2O \tag{17}$$
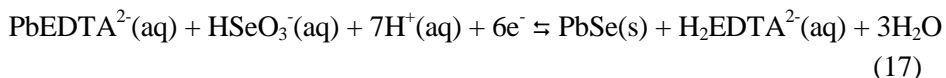
The oxidation of PbSe was found to occur by the reaction where Pb oxidises and the dissolution of Pb^{2+} causes the simultaneous detachment of Se at 0.0 V.

Deposition of Pb^0 was also studied on the Se film and it was found to deposit at much more positive potential than on the Au substrate. In addition, during the reversed scan the oxidation features characteristic to Pb oxidation were absent which confirmed that the deposited lead had formed PbSe instead of remaining as elemental lead.

4.2.2. PbTe [V]

EQCM studies on PbTe were carried out analogously to PbSe. Also the results were rather similar although the electrochemistry of TeO_3^{2-} in the alkaline pH

was found to be more complicated than that of $HSeO_3^-$ in the acidic solution (cf. above). EQCM measurements from the TeO_3^{2-} solution were made on three different surfaces; bare Au, previously deposited Te, and PbTe. The UPD reduction of TeO_3^{2-} on Au begins at -0.4 V. The bulk reduction of TeO_3^{2-} starts at the potential -0.5 V, and the four electron reduction reaction (18) was observed between -0.5–-0.7 V.

$$TeO_3^{2-}(aq) + 3H_2O + 4e^- \leftrightarrows Te(s) + 6OH^-(aq) \qquad (18)$$

Between -0.7 and -0.9 V the frequency of the QCM decreased fast as compared with the charge consumed. The stripping began at -0.9 V by a reaction:

$$Te(s) + H_2O + 2e^- \leftrightarrows HTe^-(aq) + OH^-(aq) \qquad (19)$$
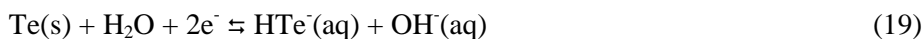
The fast frequency decrease at about -0.8 V was observed both on the Au surface and on the PbTe film, but not on the Te film. Constant potential experiments showed that at -0.7 V Te forms a dense film on Au and PbTe while at -0.85 V it deposits as loose powder. Therefore it was concluded that the fast decrease in the QCM frequency between -0.7–-0.9 V in the cyclic measurements was due to the change in the deposit morphology. That may cause an inclusion of the solvent during the deposition. Another factor which affects the crystal frequency is that the formation of a powdery film on the substrate increases the roughness of the crystal surface. The formation of powdery, dendritic or rough tellurium deposit has been observed also in the literature. [180] That study was carried out in an acidic solution and the observations differed perceptibly from ours. Powdery tellurium was observed to deposit during the forward (from positive to negative) scan in the cyclic voltammogram. During the reversed scan, dense Te formed, and it did not reduce further to H_2Te though the potential was again made more negative. Powdery tellurium, on the other hand, readily reduced further.

In our study at -0.8 V the deposition process changed on the PbTe and Au surfaces and the reduction product was completely powdery and not adhesive at all. It is notable that the change in the tellurium deposition process and the formation of powdery Te did not affect the composition of the PbTe films which was constant over the whole potential range.

PbEDTA^{2-} behaved very similarly at pH 9.0 as at pH 3.5. Only the reduction potential was somewhat more negative, -1.05 V.

Similarly to PbSe, the formation of PbTe occurs by a six electron reduction reaction (20):

$$PbEDTA^{2-}(aq) + TeO_3^{2-}(aq) + 4H_2O + 6e^- \leftrightarrows PbTe(s) + HEDTA^{3-}(aq) + 7OH^-(aq) \tag{20}$$
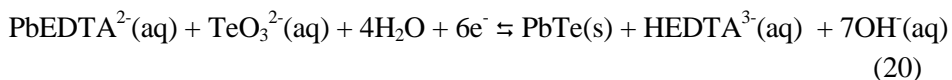
The reaction occurs between -0.65–-0.85 V. The oxidation of PbTe differed from the oxidation of PbSe since it appeared to begin at about -0.5 V with the oxidation of lead without simultaneous detachment of tellurium. The oxidation continued at 0.04 V with the simultaneous oxidation of Te.

Lead was found to deposit on a tellurium film at much more positive potential than on the Au substrate. During the reversed scan the oxidation features resembled the system which contained both Pb and Te precursors instead of Pb alone which confirmed that the deposited lead formed mostly PbTe instead of an elemental film.

In summary from the film growth and EQCM results, it is concluded that the electrodeposition processes of PbSe and PbTe occur by means of the induced codeposition mechanism in which the reduction of chalcogen, selenium or tellurium, induces the reduction of lead. The film forms at much more positive potentials than where lead reduces alone. Wide potential ranges where films with constant composition may be deposited were found. The reaction is six electron reduction and it involves first the reduction of selenium or tellurium which then induces the reduction of lead to form PbSe or PbTe. Another possibility could be the reaction between H_2Se or HTe^- and PbEDTA^{2-} but that is not probable at least at the most positive potentials, since formation of neither H_2Se nor HTe^- was observed at these potentials. In the film growth experiments, the larger the concentration of PbEDTA^{2-}, the wider the potential range where constant composition products were deposited. In addition, in EQCM studies it was evidenced that Pb reduces on top of Se and Te films forming PbSe or PbTe film instead of forming a Pb layer over the chalcogen layer.

EDTA was found to be very suitable for complexing lead. Although the use of EDTA was necessary in order to avoid spontaneous precipitation reactions, it was also otherwise practical since it moved the reduction potential of Pb to more negative potential, thereby widening the potential range for the compound deposition. On the other hand, the reduction potential of PbEDTA^{2-} was not too negative to be interfered by the reduction of hydrogen, since the overpotential for the hydrogen reduction is very large during the reduction of lead in comparison with, for example, Cu, Ag, Ni and Pt. [181]

The underpotential deposition (UPD), which was observed in both Se [IV] and Te [V] studies on Au, is well known phenomenon when a few monolayers of one metal is deposited on another metal at more positive potential than its bulk deposition potential. The UPD of selenium and tellurium has been reported earlier [182] and it was also found in our Cu$_{2-x}$Se study [114].

4.2.3. PbS [VI]

Since EQCM is not applicable for such a fast cycling rates as 10 V/s used in the PbS film growth study [III], lower cycling rates of 0.1–0.01 V/s needed to be used in this work. EQCM studies were carried out at pH 8.5.

The oxidation of HS$^-$ was found to be more favourable on the Pb and PbS surfaces than on gold. The oxidation leading to PbS film formation started on both Pb and PbS at about -1.0 V. Analogously, PbEDTA^{2-} was found to reduce more easily on the PbS surface than on the Au surface. On sulfur surface, on the other hand, the reduction of lead was observed, but it was not as intensive as it was on the selenium or tellurium surfaces in the PbSe and PbTe studies. That is probably due to more insulating nature of sulfur as compared with selenium and tellurium.

The deposition of PbS occurred by two mechanisms. The first mechanism includes the reduction of PbEDTA^{2-} to elemental lead which during the oxidation reacts with HS$^-$, as presented at the beginning of the chapter 4.1 (eqs. (11) and (12)).

In the other mechanism, PbS (or Pb) surface induces the direct chemical reaction between PbEDTA^{2-} and HS$^-$ (21):

$PbEDTA^{2-}(aq) + HS^-(aq) \leftrightarrows PbS(s) + HEDTA^{3-}(aq)$ (21)

The inducing effect of Pb and PbS surfaces was proved by the observation that PbS deposited without an external current only on these surfaces but not on a Au surface. The electroless deposition was self-terminated in an hour and the thickness of the deposited film was only 10–20 nm, as calculated from the QCM frequency change. The electroless deposition mode is possible since the reduction of $PbEDTA^{2-}$ and the oxidation of HS^- occur at the same potential on a surface covered with Pb or PbS. In earlier studies the electroless deposition has been observed in the anodic deposition of PbS [107] and CdTe [24].

The electrochemical decomposition of PbS was also studied separately in the $Na(CH_3COO)$ solution. PbS was found to decompose by the reduction reaction (22) at -1.2 V.

$PbS(s) + H_2O + 2e^- \leftrightarrows Pb(s) + HS^-(aq) + OH^-(aq)$ (22)
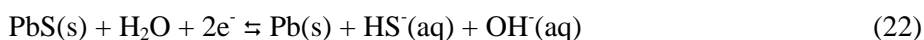
The decomposition by the oxidation begins at -0.2 V by the reaction (23)

$PbS(s) + HEDTA^{3-}(aq) + OH^-(aq) \leftrightarrows PbEDTA^{2-}(aq) + S(s) + H_2O + 2e^-$ (23)

In both cases it was probable that as the dissociation continued the whole film was detached from the surface.

4.3. Electrical measurements

4.3.1. Photoconductors

PbTe, PbSe and PbS films deposited on the Pb–acrylic foils were n-type materials as measured by the hot point probe method after removing the substrate as described in the Experimental chapter 3.3.1. The conductivity type of all the films changed as the films were annealed at 85–120 °C in air or dipped in a H_2O_2 solution. On the other hand, the conductivity type of PbTe changed from n to p also during two days storage in the deccicator without any treatments. The initially observed n-type conductivity is probably due to the n-type doping caused by the Pb under layer, because in the photovoltaic devices the surface layer of the p-type film is converted to the n-type by depositing a Pb layer on top of it. On the other hand, the hot point probe may to indicate n-type

for a high resistivity material even if the sample is weakly p-type because the method actually determines a product of a carrier concentration and a mobility. [183] The chemically deposited PbSe and PbS films are usually p-type. [152, 153, 155, 184] Also the properly sensitized films in detectors are p-type. [132]

The resistivities of the as deposited 1 µm thick PbSe, PbTe and PbS films were 1–5, 0.3–3, and 1–6 Ω cm. The resistivities of the PbTe and PbS films did not change considerably as the samples were stored in the desiccator but the resistivity of PbSe increased to 200–2 700 Ω cm during the storage. Annealing at 85 °C did not have a large effect on the resistivities (Table 7). On the other hand, at 100 °C the resistivity of PbSe increased considerably (Table 8).

Table 7. Resistivities of PbSe, PbTe and PbS samples before and after heat treatment at 85 °C in air.

Material	no. of samples	annealing time (h)	Resistivity before (Ω cm)	Resistivity after (Ω cm)
PbSe	4	16	250–2 500	90–1 500
PbSe	4	104	250–2 500	50–1 000
PbTe	2	16	2 and 3	1 and 1
PbTe	1	104	3	1
PbS	4	16	1–4	5–10
PbS	4	104	5–10	3–7

Table 8. Resistivities of PbSe, PbTe and PbS samples before and after heat treatment at 100 °C in air.

Material	no. of samples	annealing time (h)	Resistivity before (Ω cm)	Resistivity after (Ω cm)
PbSe	1	144	5	1 400
PbSe	3	168	1 000–1 500	10 500–60 000
PbSe	3	600	1 000–1 500	14 500–56 500
PbTe	2	168	1	0.5 and 1
PbTe	2	600	1	0.5 and 1
PbS	1	168	2	7
PbS	1	600	2	8

A PbTe film was also annealed at 120 °C. The resistivity increased from 0.2 to 1 Ω cm in 5 hours and from 0.2 to 2 Ω cm in 61 hours. Since the increase was not remarkable and the epoxy resin used in the sample preparation could not tolerate longer annealing times the experiments at 120 °C were not continued further. According to XRD the annealing at the temperatures studied did not affect the crystallinity of the samples.

The resistivity was observed to diminish slightly when the four point probe measurement was made under a N_2 purge, which is possibly due to the desorption of H_2O from the surface of the sample.

Since the annealing at 100 °C increased the resistivity of PbSe significantly, the D* and resistance vs. temperature measurements were made from the samples which had been annealed at 100 °C for 264 hours. Figure 8 shows resistances of PbSe films and Figure 9 those of PbS and PbTe films. Each material is represented by two or three samples, all from the same deposition and nominally similarly post treated. As typical for semiconductors, in all the films the resistivity increases as the temperature decreases.
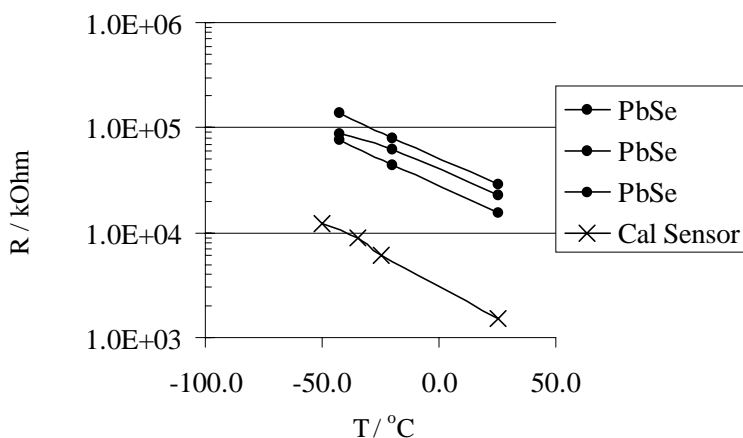
Figure 8. Resistances of electrodeposited PbSe films and a commercial PbSe film (Cal Sensor) as a function of temperature.
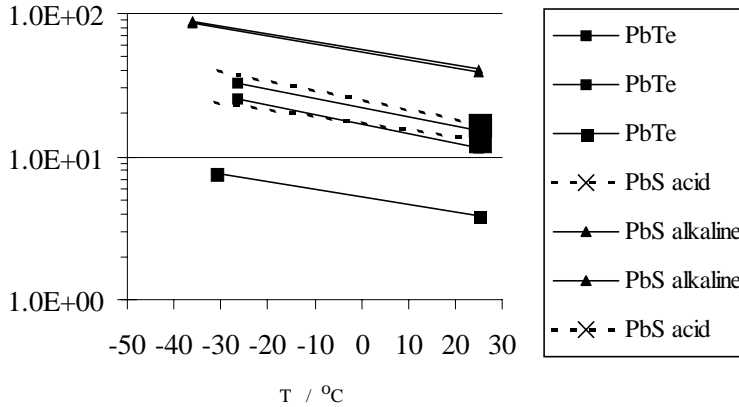
Figure 9. Resistances of electrodeposited PbS and PbTe films as a function of temperature. PbS films deposited from the acidic and alkaline solution are shown separately.

Resistances of the PbSe films are about a decade higher than those of the commercial PbSe detectors. On the other hand, the resistances of the PbS films are much smaller than those of commercial films. Comparisons are, however, difficult to make since the thicknesses of the commercial films are not known. In addition, the resistivities of the lead chalcogenide films in general vary a lot.

Resistivity changes of PbX films have in the earlier studies been proposed to be due to the oxidation of the film (cf. Chapter 2.3.3.1). On the basis of the present resistivity measurements, PbSe seems to be the most easily oxidizing but the composition changes, oxygen and hydrogen concentrations in particular, should be measured in detail by, for example, RBS, deuteron induced reactions and ERDA. The reason why PbS did not seem to oxidise is probably the structure of large cubic crystals with a limited number of grain boundaries.

D* values measured at different temperatures are presented in Figure 10. The PbTe film with the lowest resistivity in Fig. 9 is the same which has the lowest detectivity in Fig. 10. In that sample the film was not fully covered by the protecting glass plate.
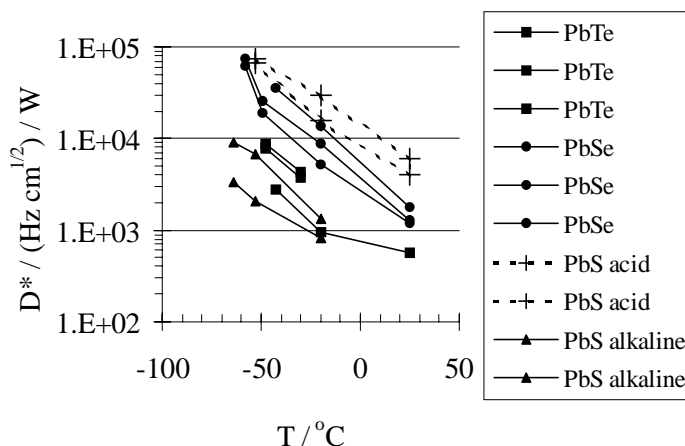
Figure 10. D (peak) values of electrodeposited films measured at different temperatures.*

Wavelength dependence of the photosensitivities of PbSe and PbS films were also measured up to the highest wavelength measurable with the equipment used and the results were compared with the commercial (Cal Sensor) PbSe and PbS films measured with the same equipment. The electrodeposited PbSe and commercial PbSe films as well as electrodeposited PbS and commercial PbS films showed very similar behaviour.

Detector time constants could not be measured. The maximum chopper frequency which could be used in the measurements was 1 kHz, so the time constants are below 1 µs. In comparison with commercial detectors (Table 4), the time constant of the electrodeposited PbS films is thus much lower.

Signal noise decreased when the temperature decreased, as typical for PbS and PbSe detectors. The signal noise of the PbTe films was around 1 µV at room temperature. In the PbS films it was close to the noise of the commercial film measured with the same equipment, about 4 µV. This means that the low D*

values of the present samples were due to a weak photosignal. In PbSe films the noise was large, over $100\,\mu V$.

D* values of the films were several decades below those of the commercial detectors and the best values presented in the earlier studies. However, the results were rather consistent and all the films showed photoactivity. In addition, the values would probably have been 0.5–1 decades larger if the sample cover glass had been more IR transparent. The D* values of other electrodeposited PbX films have not been published. The effects of annealing as well as other post deposition treatments which could sensitise the films should be studied more carefully. Unfortunately, the post deposition treatments are poorly documented. One possibility could be to try to take advantage of the sample preparation where the substrate lead film is dissolved electrochemically. PbX film could possibly be oxidised simultaneously.

The glass plate which was used on top of the photoconductive samples is possibly not able to cover the film surface effectively enough against degradation. The cover is essential as is seen from the PbTe film which was not fully covered, and it had the lowest resistance as well as the lowest detectivity (Figs. 9 and 10). Therefore a deposition of a protective film on the chalcogenide film should be considered.

4.3.2. Photovoltaic diodes

The current - voltage (I-U) curve of a photovoltaic PbSe sample measured without illumination is shown in Fig. 11. The curves of both PbSe and PbS films clearly showed diode type behaviour which denotes that a p-n junction was formed and the preparation of photovoltaic device may be possible.
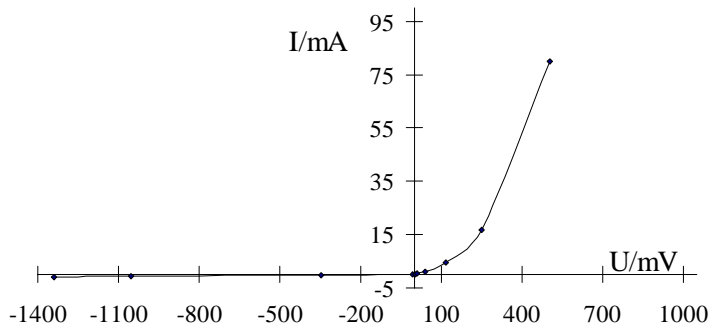
Figure 11. I-U curve of a PbSe sample.

The best D* (peak) values were 5.5×10^6 cm Hz$^{1/2}$ W^{-1} for the PbSe films and 1.6×10^6 cm Hz$^{1/2}$ W^{-1} for the PbS films. The D* values were rather low, though clearly higher than those of the photoconductors, and also in this case post deposition treatments and sample protection should be studied.

5. Conclusions

For infrared technology it is essential to manufacture IR active films, such as PbSe and PbS, by a low cost and reproducible method. In the present thesis PbSe, PbTe and PbS films were prepared by electrodeposition using two different approaches, namely constant potential (PbSe and PbTe) and cyclic (PbS) deposition.

The depositions were carried out at room temperature in aqueous solutions and EDTA was used to complex lead. As the complexing agent prevented the formation of unwanted insoluble compounds such as $PbSeO_3$ and $Pb(OH)_2$, it allowed the use of rather neutral deposition solutions; PbSe was deposited at pH 3.5, PbTe at pH 9.0 and PbS at pH 8.5. In comparison, earlier PbSe and PbTe films had been electrodeposited from 0.1 M HNO_3 solution. A drawback of very acidic deposition solutions is that H_2Se, H_2Te or H_2S form at more positive potentials. Besides being toxic, those species may also increase the amount of elemental Se, Te, or S in the films. Another drawback is the possible dissolution of substrates in highly acidic solutions. The use of EDTA also widens the deposition potential range by moving the reduction of lead to more negative potentials, and thus in the present study all materials could be deposited over wide potential ranges. The cyclic method which was used to deposit PbS films allowed to use a more stable precursor solution than before.

The films were analysed by various methods: XRD, EDX. WDX, SEM, profilometry, RBS, ERDA, and deuteron induced reactions. PbSe and PbS films were stoichiometric whereas PbTe films contained an excess of tellurium. All films contained hydrogen and oxygen impurities originating from the aqueous deposition solution. The films had polycrystalline, randomly oriented cubic structure.

Mechanistic studies on electrodeposition of PbSe, PbTe and PbS thin films were for the first time carried out using electrochemical quartz crystal microbalance combined with cyclic voltammetry. The results were well compatible with the film growth experiments. Electrodeposition of PbSe and PbTe occurs by the induced codeposition mechanism where variations in the precursor concentrations do not have large effect on the film composition. This mechanism involves a six electron overall reaction where selenium or tellurium reduces first and then induces the reduction of lead to form PbSe or PbTe. When

Pb was deposited on top of a previously deposited Se or Te film it formed PbSe or PbTe compounds instead of elemental lead. The cyclic electrodeposition of PbS, on the other hand, includes several simultaneous processes, which are difficult to distinguish by EQCM. On more general level, EQCM results confirmed the earlier findings on the electrochemistry of Pb, S, Se and Te but also new information was obtained.

Electrical properties of the PbS, PbSe and PbTe films were studied briefly. Photoconductive samples were made from all materials and photovoltaic diode samples from PbSe and PbS films. Before measurements photoconductive samples were annealed at 100 °C in air, which increased the resistance of PbSe from about 20 kΩ to 10 MΩ whereas the resistances of PbS and PbTe films remained between 10 kΩ – 100 kΩ. All materials, both photoconductive and photovoltaic samples showed IR activity. It is concluded that the preparation of both photoconductive and photovoltaic IR detectors might be possible by electrodeposition but thorough studies on the post deposition treatments as well as sample preparation are still needed.

References

1. Brenner. A. Electrodeposition of Alloys, Academic Press, New York, 1963. 677 p.

2. Gobrecht, H., Liess, H.D. and Tausend, A. Elektrochemische Abscheidung von Metallseleniden. Ber. Bunsen–Ges., 67 (1963), p. 930.

3. Kröger, F.A. Cathodic deposition and characterisation of metallic or semiconducting binary alloys or compounds. J. Electrochem. Soc., 125 (1978), p. 2028.

4. Panicker, M. P. R., Knaster, M. and Kröger, F. A. Cathodic deposition of CdTe from Aqueous Electrolytes. J. Electrochem. Soc., 125 (1978), p. 566.

5. Milazzo, G. and Caroli, S. (eds.). Tables of Standard Electrode Potentials. John Wiley & Sons, Chichester, 1978.

6. Lide, D. R. (ed. in chief). CRC Handbook of Chemistry and Physics. 77th ed, 1996–1997, Boca Raton.

7. Gregory, B.W. and Stickney, J.L. Electrochemical atomic layer epitaxy (ECALE). J. Electroanal. Chem., 300 (1991), p. 543.

8. Rajeshwar, K. Electrosynhesized thin films of group II-VI compound semiconductors, alloys and superstructures. Adv. Mater., 4 (1992), p. 23.

9. Kemell, M., Ritala, M., Saloniemi, H., Leskelä, M., Rauhala, E. and Sajavaara, T. One-step electrodeposition of $Cu_{2-x}Se$ and $CuInSe_2$ thin films by the induced co-deposition mechanism. J. Electrochem. Soc., 147 (2000), p. 1080.

10. Hantke, G. (ed.). Gmelin Handbuch der Anorganishen Chemie 8. Vol. 11 B 1. Verlag Chemie Gmbh., Berlin, 1976. P. 58.

11. Kampmann, A., Cowache, P., Vedel, J. and Lincot, D. Investigation of the influence of the electrodeposition potential on the optical, photoelectrochemical and structural properties of as-deposited CdTe. J. Electroanal. Chem., 387 (1995), p. 53.

12. Sella, C., Boncorps, P. and Vedel, J. The electrodeposition mechanism of CdTe from acidic squeous solutions. J. Electrochem. Soc., 133 (1986), p. 2043.

13. Murase, K., Uchida, H., Hirato, T. and Awakura, Y. Electrodeposition of CdTe films from ammoniacal alkaline aqueous solution at low cathodic overpotentials. J. Electrochem. Soc., 146 (1999), p. 531.

14. Murase, K., Watanabe, H., Hirato, T. and Awakura, Y. Potential-pH diagram of the Cd-Te-NH$_3$-H$_2$O system and electrodeposition behavior of CdTe from ammoniacal alkaline baths. J. Electrochem. Soc., 146 (1999), p. 1798.

15. Murase, K., Watanabe, H., Mori, S., Hirato, T. and Awakura, Y. The electrodeposition mechanism of CdTe from acidic aqueous solutions. J. Electrochem. Soc., 146 (1999), p. 4477.

16. Meulenkamp, E.A. and Peter, L.M. Mechanistic aspects of the electrodeposition of stoichiometric CdTe on semiconductor substrates. J. Chem. Soc., Faraday Trans., 92 (1996), p. 4077.

17. Cowache, P., Lincot, D. and Vedel, J. Cathodic electrodeposition of CdTe on conducting glass. J. Electrochem. Soc., 136 (1989), p. 1646.

18. Rastogi, A.C. and Balakrishnan, K.S. Monocrystalline CdTe thin films by electrochemical depostion from aprotic electrolytes. J. Electrochem. Soc., 136 (1989), p. 1502.

19. Lincot, D., Kampmann, A., Mokili, B., Vedel, J., Cortes, R. and Froment, M. Epitaxial electrodeposition of CdTe films on InP from aqueous solutions: Role of a chemically deposited CdS intermediate layer. Appl. Phys. Lett., 67 (1995), p. 2355.

20. Cocivera, M., Darkowski, A. and Love, B. Thin film CdSe electrodeposited from selenosulfite solution. J. Electrochem. Soc., 131 (1984), p. 2514.

21. Skyllas-Kazacos, M. and Miller, B. Electrodeposition of CdSe films from selenosulfite solution. J. Electrochem. Soc., 127 (1980), p. 2378.

22. Skyllas-Kazakos, M. Electrodeposition of CdSe and CdTe thin films from cyanide solutions. J. Electroanal. Chem., 148 (1983), p. 233.

23. Ham, D., Mishra, K.K. and Rajeshwar, K. Anodic electrosynthesis of CdSe thin films. J. Electrochem. Soc., 138 (1991), p. 100.

24. Ham, D., Mishra, K.K, Weiss, A. and Rajeshwar, K. Anodic electrosynthesis of CdTe thin films. Chem. Mat., 1 (1989), p. 619.

25. Rastogi, A.C. and Balakrishnan, K.S. Growth, structure and composition of electrodeposited thin films for solar cells. Sol. Energy Mater. Sol. Cells, 36 (1995), p. 121.

26. Bouroushian, M., Loizos, Z., Spyrellis, N. and Maurin, G. Hexagonal cadmium chalcogenide thin films prepared by electrodeposition from near-boiling aqueous solutions. Appl. Surf. Sci., 115 (1997), p. 103.

27. Darkowski, A. and Cocivera, M. Electrodeposition of CdTe using phosphine telluride. J. Electrochem. Soc., 132 (1985), p. 2768.

28. Sanders, B.W. and Cocivera, M. Characterization of CdSe electrodeposited from diethylene glycol solution containing tri-n-butylphosphine selenide. J. Electrochem. Soc., 134 (1987), p. 1075.

29. Morris, G.C. and Vanderveen, R.J. Solar cells from thin films prepared by periodic pulse electrodeposition. Appl. Surf. Sci., 92 (1996), p. 630.

30. Fatas, E., Herrasti, P., Arjona, F. and Camarero, E.G. Characterization of CdS thin films electrodeposited by an alternating current electrolysis method. J. Electrochem. Soc., 134 (1987), p. 2799.

31. Moorthy Babu, S., Dhanasekaran, R. and Ramasamy, P. Electrodeposition of CdTe by potentiostatic and periodic pulse techniques. Thin Solid Films, 202 (1991), p. 67.

32. Murali, K.R., Subramanian, V., Rangerajan, N., Lakshmanan, A.S. and Rangerajan, S.K. Photoelectrochemical studies on pulse plated CdSe films. J. Electroanal. Chem., 303 (1991), p. 261.

33. Kressin, A.M., Doan, V.V., Klein, J.D. and Sailor, M.J. Synthesis of stoichiometric cadmium selenide films via sequential monolayer electrodeposition. Chem. Mater., 3 (1991), p. 1015.

34. Jackson, F., Berlouis, L.E.A. and Rocabois, P. Layer-by-layer electrodeposition of CdTe onto silicon. J. Cryst. Growth, 159 (1996), p. 200.

35. Baranski, A.S. and Fawsett, W.R. The electrodeposition of metal chalcogenides. J. Electrochem. Soc., 127 (1980), p. 766.

36. Baranski, A.S., Bennet, M.S. and Fawsett, W.R. The physical properties of CdS thin films electrodeposited from aqueous diethylene glycol solutions. J. Appl. Phys., 54 (1983), p. 6390.

37. Fatas, E. and Herrasti, P. Voltammetric study of the electrodeposition of CdS films from propylene carbonate solutions. Electrochim. Acta, 33 (1988), p. 959.

38. Lokhande, C.D., Patil, P.S., Yermune, V.S. and Pawar, S.H. Electrodeposition of Ag_2S films from aqueous bath. Bull. Electrochem., 6 (1990), p. 842.

39. Zainal, Z., Hussein, M.Z., Kassim, A. and Ghazali, A. Electrodeposited SnS thin films from aqueous solution. J. Mater. Sci. Lett., 16 (1997), p. 1446.

40. Ghazali, A., Zainal, Z., Hussein, M.Z. and Kassim, A. Cathodic electrodeposition of SnS in the presence of EDTA in aqueous media. Sol. Energy Mat. Sol. Cells, 55 (1998), p. 237.

41. Engelken, R.D. and McCloud, H.E. Electrodeposition and materials characterization of Cu_xS Films. J. Electrochem. Soc., 132 (1985), p. 567.

42. Yesugade, N.S., Lokhande, C.D. and Bhosale, C.H. Structural and optical properties of electrodeposited Bi_2S_3, Sb_2S_3 and As_2S_3 thin films. Thin Solid Films, 263 (1995), p. 145.

43. Mohite, U.K. and Lokhande, C.D. Electrosynthesis of yttrium chalcogenides from a non-aqueous bath. Appl. Surf. Sci., 92 (1996), p. 151.

44. Saksena, S., Pandya, D.K. and Chopra, K.L. Electroconversion of CdS to Cu_xS for thin film solar cells. Thin Solid Films, 94 (1982), p. 223.

45. Neumann-Spallart, M. and Köningstein, C. Electrodeposition of zinc telluride. Thin Solid Films, 265 (1995), p. 33.

46. Königstein, C. and Neumann-Spallart, M. Mechanistic studies on the electrodeposition of ZnTe. J. Electrochem. Soc., 145 (1998), p. 337.

47. Samantilleke, A.P., Boyle, M.H., Young, J. and Dharmadasa, I.M. Electrodeposition of n-type and p-type ZnSe thin films for applications in large area optoelectronic devices. J. Mat. Sci., Mat. Electron., 9 (1998), p. 289.

48. Bozzini, B., Baker, M.A. Cavallotti, P.L., Cerri, E. and Lenardi, C. Electrodeposition of ZnTe for photovoltaic cells. Thin Solid Films, 361–362 (2000), p. 388.

49. Baranski, A.S., Fawsett, W.R. and Gilbert, C.M. The structural and compositional characterisation of bismuth sulfide films grown by cathodic deposition. J. Electrochem. Soc., 130 (1983), p. 2423.

50. Adachi, A., Kudo, A. and Sakata, T. The optical and photoelectrochemical properties of electrodeposited CdS and SnS thin films. Bull. Chem. Soc. Jpn., 68 (1995), p. 3283.

51. Mishra, K.K., Rajeshwar, Weiss, A., Murley, M., Engelken, R.D., Slayton, M. and McCloud, H.E. Electrodeposition and Characterization of SnS Thin Films. J. Electrochem. Soc., 136 (1989), p. 1915.

52. Chaure, N.B., Nair, J.P. Jayakrishnan, R., Ganesan, V. and Pandey, R.K. Effect of Cu-doping on the morpholology of ZnTe films electrodeposited from nonaqueous bath. Thin Solid Films, 324 (1998), p. 78.

53. Chaure, N.B., Jayakrishnan, R., Nair, J.P. and Pandey, R.K. Electrodeposition of ZnTe films from a nonaqueous bath. Semicond. Sci. Technol., 12 (1997), p. 1171.

54. Chandra, S., Srivastava, O.N. and Sahu, S.N. Electrodeposited tungsten selenide films 1. Preparatory technique and structural characterization. Phys. Stat. Sol., (a) 88 (1985), p. 497.

55. de Tacconi, N.R., Medvedko, O. and Rajeshwar, K. Cathodic electrosynthesis of metal sulphide thin films at a sulphur-modified gold surface: application to the iron sulphide system. J. Electroanal. Chem., 379 (1994), p. 545.

56. de Tacconi, N.R. and Rajeshwar, K. Electrosynthesis of indium sulfide on sulfur-modified polycrystalline gold electrodes. J. Electroanal. Chem., 444 (1998), p. 7.

57. Ponomarev, E.A., Neumann-Spallart, M., Hodes, G. and Lévy-Clément, C. Electrochemical deposition of MoS_2 thin films by reduction of tetrathiomolybdate. Thin Solid Films, 280 (1996), p. 86.

58. Ponomarev, E.A., Albu-Yaron, A., Tenne, R. and Lévy-Clément, C. Electrochemical deposition of quantized particle MoS_2 thin films. J. Electrochem. Soc., 144 (1997), p. L277.

59. Albu-Yaron, A., Lévy-Clément, C. and Hutchison, J.L. A study on MoS2 thin films electrochemically deposited in ethylene glycol at 165°C. Electrochem. Solid-State Lett., 2 (1999), p. 627.

60. Miller, B. and Heller, A. Semiconductor liquid junction solar cells based on anodic sulphide films. Nature, 262 (1976), p. 680.

61. Peter, L.M. The photoelectrochemical properties of anodic Bi_2S_3. J. Electroanal. Chem., 98 (1979), p. 49.

62. Schimmel, MI., de Tacconi, N.R. and Rajeshwar, K. Anodic Synthesis of Cu_2S and $CuInS_2$ films. J. Electroanal. Chem., 453 (1998), p. 187.

63. Scharifker, B., Rugeles, R. and Mozota, J. Electrocrystallization of copper sulphide Cu_2S on copper. Electrochim. Acta, 29 (1984), p. 261.

64. Vasquez Moll, D., de Chalvo, M.R.G., Salvarezza, R.C. and Arvia, A.J. Corrosion and passivity of copper in solutions containing sodium sulphide. Analysis of potentiostatic current transits. Electrochim. Acta, 30 (1985), p. 1011.

65. Yukawa, T., Kuwabara, K. and Koumoto, K. Electrodeposition of $CuInS_2$ from aqueous solutions. Part I. Electrodeposition of Cu-S film. Thin Solid Films, 280 (1996), p. 160.

66. Sahu, S.N. and Sanchez, C. Preparation of Fe_xS_y thin films by an electrodeposition technique. J. Mater. Sci. Lett., 11 (1992), p. 1540.

67. Viechbeck, A. and Hackerman, N. Formation and reduction of anodic sulfide films on antimony electrodes. J. Electrochem. Soc., 131 (1984), p. 1315.

68. Ichimura, M., Takeuchi, K., Ono, Y. and Arai, E. Electrochemical deposition of SnS thin films. Thin Solid Films, 361–362 (2000), p. 98.

69. Mahalingam, T. and Sanjeeviraja, C. Characterzation of electrodeposited ZnS thin films. Phys. Stat. Sol., (a) 129 (1992), p. K89.

70. Lokhande, C.D., Jadhav, M.S. and Pawar, S.H. Electrodeposition of ZnS films from an alkaline bath. J. Electrochem. Soc., 136 (1989), p. 2756.

71. Torane, A.P., Lokhande, C.D., Patil, P.S. and Bhosale, C.H. Preparation and characterization of electrodeposited Bi_2Se_3 thin films. Mater. Chem. Phys., 55 (1998), p. 51.

72. Bhattacharya, R.N., Fernandez, A.M., Contreras, M.A., Keane, J., Tennant, A.L., Ramanathan, K., Tuttle, J.R., Noufi, R.N. and Hermann, A.M. Electrodeposition of In-Se, Cu-Se and Cu-In-Se thin films. J. Electrochem. Soc., 143 (1996), p. 854.

73. Lokhande, C.D. Electrodeposition of semiconductor layers of In-Se, Cu-Se and Cu-In-Se. Bull. Electrochem., 3 (1987), p. 219.

74. Thouin, L., Rouquette-Sanchez, S. and Vedel, J. Electrodeposition of copper-selenium binaries in citric acid medium. Electrochim. Acta, 38 (1993), p. 2387.

75. Lippkow, D. and Strehblow, H.-H. Structural investigations of thin films of copperselenide electrodeposited at elevated temperatures. Electrochim. Acta, 43 (1998), p. 2131.

76. Massaccesi, S., Sanchez, S. and Vedel, J. Electrodeposition of indium selenide In_2Se_3. J. Electroanal. Chem., 412 (1996), p. 95.

77. Igasaki, Y. and Fujiwara, T. Preparation of highly oriented InSe films by electrodeposition. J. Cryst. Growth, 158 (1996), p. 268.

78. Fujiwara, T. and Igasaki, Y. The effects of pulsing the current in galvanostatic electrodeposition technique on the composition and surface morphology of In-Se films. J. Cryst. Growth, 178 (1997), p. 321.

79. Chandra, S. and Sahu, S.N. Electrodeposited semiconducting molybdenum selenide films: 1. Preparatory technique and structural characterization. J. Phys. D: Appl. Phys., 17 (1984), p. 2115.

80. Chandra, S. and Sahu, S.N. Electrodeposited semiconducting molybdenum selenide films: 2. Optical, electrical, electrochemical and photoelectrochemical solar cell studies. J. Phys. D: Appl. Phys., 17 (1984), p. 2125.

81. Torane, A.P., Rajpure, K.Y. and Bhosale, C.H. Preparation and characterization of electrodeposited Sb_2Se_3 thin films. Mater. Chem. Phys., 61 (1999), p. 219.

82. Fernández, A.M. and Merino, M.G. Preparation and characterization of Sb_2Se_3 thin films prepared by electrodeposition for photovoltaic applications. Thin Solid Films, 366 (2000), p. 202.

83. Engelken, R.D., Berry, A.K., Van Doren, T.P., Boone, J.L. and Shahnazary, A. Electrodeposition and analysis of tin selenide films. J. Electrochem. Soc., 133 (1986), p. 581.

84. Subramanian, B., Mahalingam, T., Sanjeeviraja, C., Jayachandran, M. and Chockalingam, M.J. Electrodeposition of Sn, Se, SnSe and the material properties of SnSe films. Thin Solid Films, 357 (1999), p. 119.

85. Wei, C. and Rajeshwar, K. Flow electrosyntheses of group II–VI compound semiconductor thin films and composition-modulated superstructures. J. Electrochem. Soc., 139 (1992), p. L40.

86. Chandramohan, R., Sanjeeviraja, C. and Mahalingam, T. Preparation of zinc selenide thin films by electrodeposition technique for solar cell applications. Phys. Stat. Sol., (a) 163 (1997), p. R11.

87. Natarajan, C., Sharon, M., Lévy-Clément, C. and Neumann-Spallart, M. Electrodeposition of zinc selenide. Thin Solid Films, 237 (1994), p. 118.

88. Singh, K. and Rai, J.P. Electrosynthesis of polycrystalline photo-electroactive p-zinc selenide. J. Mat. Sci. Lett., 4 (1985), p. 1401.

89. Singh, K. and Rai, J.P. Electrosynthesis and photoelectroactivity of polycrystalline p-zinc selenide. Phys. Stat. Sol., (a) 99 (1987), p. 257.

90. Magri, P., Boulangeer, C. and Lecuire, J.-M. Synthesis, properties and performances of electrodeposited bismuth telluride films. J. Mater. Chem., 6 (1996), p. 773.

91. Takahashi, M., Katou, Y., Nagata, K. and Furuta, S. The composition and conductivity of electrodeposited Bi-Te alloy films. Thin Solid Films, 240 (1994), p. 70.

92. Gerritsen, H.J. Electrochemical deposition of photosensitive CdTe and ZnTe on Tellurium. J. Electrochem. Soc., 131 (1984), p. 136.

93. Baoming, H.M., Lister, T.E. and Stickney, J.L. Electrochemical epitaxy. In: The Handbook of Surface Imaging and Visualization, Hubbard, A.T. (ed.). CRC Press, Boca Raton, 1995. P. 75.

94. Peulon, S. and Lincot, D. Cathodic eletrodeposition from aqueous solution of dense of open-structured zinc oxide films. Adv. Mater., 8 (1996), p. 166.

95. Bohannan, E.W., Shumsky, M.G. and Switzer, J.A. Epitaxial electrodeposition of copper(I) oxide on single-crystal gold(100). Chem. Mater., 11 (1999), p. 2289.

96. Velichenko, A.B., Girenko, D.V. and Danilov, F.I. Mechanism of PbO_2 electrodeposition. J. Electroanal. Chem., 405 (1996), p. 127.

97. Gal-Or, L., Silberman, I. and Chaim, R. Electrolytic ZrO_2 coatings. J. Electrochem. Soc., 138 (1991), p. 1939.

98. Therese, G.H.A. and Kamath, P.V. Electrochemical synthesis of metal oxides and hydroxides. Chem. Mater., 12 (2000), p. 1195.

99. Strelsov, E.A., Osipovich, N.P., Ivashkevich, L.S., Lyakhov, A.S. and Sviridov, V.V. Electrochemical deposition of PbSe, PbTe and PbSeTe films. Russ. J. Appl. Chem., 70 (1997), p. 1651.

100. Strelsov, E.A., Osipovich, N.P., Ivashkevich, L.S., Lyakhov, A.S. and Sviridov, V.V. Electrochemical deposition of PbSe films. Electrochim. Acta, (1997), p. 869.

101. Strelsov, E.A., Osipovich, N.P., Lyakhov, A.S. and Ivashkevich, L.S. Electrodeposition of metal sulfide superlattices. Inorg. Mat., 33 (1997), p. 442.

102. Molin, A.N. and Dikusar, A.I. Electrochemical deposition of PbSe thin films from aqueous solutions. Thin Solid Films, 265 (1995), p. 3.

103. Sharon, M., Ramaiah, K.S., Kumar, M., Neumann-Spallart, M. and Levy-Clement, C. Electrodeposition of lead sulphide in acidic medium. J. Electroanal. Chem., 436 (1997), p. 49.

104. Takahashi, M., Ohshima, Y. Nagata, K. and Furuta, S. Electrodeposition of PbS films from acidic solution. J. Electroanal. Chem., 359 (1993), p. 281.

105. Vertegel, A.A., Shumsky, M.G. and Switzer, J.A. Epitaxial electrodeposition of lead sulfide on (100) oriented single-crystal growth. Angew. Chem. Int. Ed. Eng, 38 (1999), p. 3169.

106. Scharifker, B. and Ferreira, F. and Mozota, J. Electrodeposition of lead sulphide. Electrochim. Acta, 5 (1985), p. 677.

107. Totland, K.M. and Harrington, D.A. Anodic phase formation on lead amalgam electrodes in sodium sulfide solution. J. Electroanal. Chem., 274 (1989), p. 61.

108. Miles, M.H. and McEwan, W.S. Electrolytic synthesis of some heavy metal tellurides. J. Electrochem. Soc., 120 (1973), p. 1069.

109. Buttry, D. A. and Ward, M. D. Measurement of interfacial processes at electrode surfaces with the EQCM. Chem. Rev., 92 (1992), p. 1355.

110. Buttry D.A. Application of the electrochemical quartz crystal microbalance to electrochemistry. In: Electroanalytical Chemistry. A Series of Advances. Bard, A.J. (ed.). Vol. 17, Marcel Dekker, New York, 1991, p.1.

111. Wei, C., Bose, C.S.C. and Rajeshwar, K. Compositional analysis of electrosynthesized semiconductor thin films by EQCM: application to the Cd + Se system. J. Electroanal. Chem., 327 (1992), p. 331.

112. Myung, N., Jun, J.H., Ku, H.B., Chung, H.K. and Rajeshwar, K. Application of combined flow injection-electrochemical quartz crystal microgravity to on-line electrodeposition and compositional analysis of CdSe thin films. Microchem. J., 62 (1999), p. 15.

113. Marlot, A. and Vedel, J. Electrodeposition of copper-selenium compounds onto gold using a rotating electrochemical quartz crystal microbalance. J. Electrochem. Soc., 146 (1999), p. 177.

114. Kemell, M., Saloniemi, H., Ritala, M. and Leskelä M. Electrochemical quartz crystal microbalance study of the electrodeposition mechanism of $Cu_{2-x}Se$ thin films. Electrochim. Acta, 45 (2000), p. 3737.

115. Kemell, M., Saloniemi H., Ritala, M. and Leskelä, M. Electrochemical quarzt crystal microbalance study of the electrodeposition mechanism of $CuInSe_2$ thin films. J. Electrochem. Soc. submitted.

116. Mori, E., Baker, C.K. Aqueous electrochemistry of tellurium at glassy carbon and gold. Reynolds, J.R. and Rajeswar, K., J. Electroanal. Chem., 252 (1988), p. 441.

117. Wei, C., Myung, N. and Rajeshwar, K. In situ compositional analysis of electrosynthesized cadmium telluride thin films by electrochemical quartz crystal microgravimetry. J. Electroanal. Chem., 347 (1993), p. 223.

118. Matias, J.G.N., Julião, J.F., Soares, D.M. and Gorenstein, A. CdTe electrodeposition and stripping – an electrochemical quartz crystal analysis. J. Electroanal. Chem., 431 (1997), p. 163.

119. Kothiyal, G.P. and Ghosh, B. On conductivity in lead chalcogenides. Prog. Cryst. Growth Charact., 20 (1990), p. 313.

120. Ito, M., Seo, W-S. and Koumoto, K., J. Mater. Res. Thermoelectroc properties of PbTe thin films prepared by gas evaporation method. 14 (1999), p. 209.

121. Martin, J.M., Hernández, L., Adell, I., Rodriguez, A. and Lopez, F. Arrays of thermally evaporated PbSe infrared photodetectors deposited on Si substrate operating at room temperature. Semicond. Sci. Technol., 11 (1996), p. 1740.

122. Zogg, H., Vogt, W. and Melchior, H. Heteroepitaxial IV–VI infrared sensors on Si-substrates with fluoride buffer layers. Nucl. Instrum. Methods Phys. Res., A253, (1987), p. 418.

123. Zogg, H., Blunier, S., Hoshino, T., Maissen, C., Mesek, J. and Tiwari, A.N. Infrared Sensors Arrays with 3.12 um Cutoff Wavelengths in Heteoepitaxial Narrow-Gap Semiconductors on Silicon Substrates. IEEE Trans. Electron Dev., 38 (1991), p. 1110.

124. Zogg, H., Fach, A., John, J., Masek, J., Müller, P., Paglino, C. and Blunier, S. Photovoltaic IV–VI on Si infrared sensor arrays for thermal imaging. Opt. Eng., 34 (1995), p. 1964.

125. Collot, P., Nguyen-Van-Dau, F. and Mathet, V. Monolithic integration of PbSe IR photodiodes on Si substrates for near ambient temperature operation. Semicond. Sci. Technol., 9 (1994), p. 1133.

126. Yang, Y., Li, W., Yu, L., Sun, X., Xu, L. and Hou, L. Novel infrared detector. Infrared Phys. Technol., 38 (1997), p. 9.

127. Corsi, C. Infrared detector arrays by new technologies. Proc. IEEE, 63 (1975), p. 14.

128. Fainer, N.I., Kosinova, M.L., Rumyantsev, Y.M., Salman, E.G. and Kuznetsov, F.A. Growth of PbS and CdS thin films by low-pressure chemical vapour deposition using dithiocarbamates. Thin Solid Films, 280 (1996), p. 16.

129. Trinidade, T. and O'Brien, P. Lead dithiocarbamato complexes as precursors for the LP-MOCVD of lead sulfide. Chem. Vap. Deposition, 3 (1997), p. 75.

130. Leskelä, M., Niinistö, L., Niemelä, P., Nykänen, E., Soininen, P., Tiitta, M. and Vähäkangas, J. Preparation of PbS thin films by the ALE process. Vacuum, 41 (1990), p. 1457.

131. Nykänen, E., Laine-Ylijoki, J., Soininen, P., Niinistö, L., Leskelä, M. and Hubert-Pfalzgraf, L.G. Growth of PbS thin films from novel precursors by ALE. J. Mater. Chem., 4 (1994), p. 1409.

132. Johnson, T.H. Lead salt detectors and arrays PbS and PbSe. Proc. SPIE Int. Soc. Opt. Eng., 443 (1984), p. 60.

133. Hauser, O. and Biesalski, E. Einfache Herstellung von Metallsulfidspiegeln. Chem. Zeit., 121 (1910), p. 1079.

134. Davis, J.L. and Norr, M.K. Ge-Epitaxial-PbS heterojunctions. J. Appl. Phys., 37 (1966), p. 1670.

135. Sigmund, H. and Berchtold, K. Electrical and Photovoltaic Properties of PbS-Si heterodiodes. Phys. Stat. Sol., (a) 20 (1967), p. 255.

136. Watanabe, S. and Mita, Y. CdS-PbS heterojunctions. J. Electrochem. Soc., 116 (1969), p. 989.

137. Sharma, B.L. and Mukerjee, S.N. PbS-GaAs heterojunctions. Phys. Stat. Sol., (a) 2 (1970), p. K21.

138. Guizzetti, G., Filippini, F., Reguzzoni, E. and Samoggia, G. Electrical properties and spectral response of PbS-Ge heterojunctions. Phys. Stat. Sol., (a) 6 (1971), p. 605.

139. Watanabe, S. and Mita, Y. Electrical properties of CdS-PbS heterojunctions. Solid-State Electron., 15 (1972), p. 5.

140. Bernabucci, F., Margaritondo, G., Migliorato, P. and Perfetti, P. Electrical properties and Spectral response of PbS-Ge heterojunctions. Phys.Stat. Sol. (a) 15 (1973), p. 621.

141. Elabd, H. and Steckl, A.J. Growth of polycrystalline PbS films. J. Vac. Sci. Technol., 15 (1978), p. 264.

142. Elabd, H. and Steckl, A.J. Structural and compositional properties of the PbS-Si heterojunction. J. Appl. Phys., 51 (1980), p. 726.

143. Isshiki, M., Endo, T., Masumoto, K. and Usui, Y. Epitaxial growth of PbS thin films from aqueous solution. J. Electrochem. Soc., 137 (1990), p. 2697.

144. Rahnamai, H. and Zemel, J.N. The thin film thickness dependence of the space charge capacitance in PbS-Si heterojunctions. Thin Solid Films, 69 (1980), p. L19.

145. Rahnamai, H., Gray, H.J. and Zemel, J.N. The PbS-Si heterojunction. I: Growth and structure of PbS films on silicon. Thin Solid Films, 69 (1980), p. 347.

146. Rahnamai, H. and Zemel, J.N. The PbS-Si heterojunction II: Electrical properties. Thin Solid Films, 74 (1980), p. 17.

147. Rahnamai, H. and Zemel, J.N. The PbS-Si heterojunction III: Optical properties. Thin Solid Films, 74 (1980), p. 23.

148. Nair, P.K., Nair, M.T.S., Fernandez, A. and Ocampo, M. Prospects of chemically deposited metal chalcogenide thin films for solar control applications. J. Phys. D: Appl. Phys., 22 (1989), p. 829.

149. Nair, P.K. and Nair, M.T.S.Versatile solar control characteristics of chemically deposited PbS-Cu$_x$S thin film combinations. Semicond. Sci. Technol., 4 (1989), p. 807.

150. Nascu, C., Vomir, V., Pop, I., Ionescu,V. and Grecu, R. The study of PbS films: Influence of oxidants on the chemically deposited PbS thin films. Mater. Sci. Eng., B41 (1996), p. 235.

151. Pop, I., Ionescu, V., Nascu, C., Vomir, V., Grecu, R. and Indrea, E. The study of PbS films: the behaviour at low temperature thermal treatment. Thin Solid Films, 283 (1996), p. 119.

152. Basu, P.K., Chaudhuri, T.K., Nandi, K.C., Saraswat, R.S. and Acharya, H.N. Preparation and characterisation of chemically deposited lead sulphide thin films. J. Mater. Sci., 25 (1990), p. 4014.

153. Cândea, R.M., Turcu, R., Borodi, G. and Bratu, I. Effects of thermal annealing in air on VE, COD and CAD PbSe films. Phys. Stat. Sol., (a) 100 (1987), p. 149.

154. Zingaro, R.A. and Skolvin, D.O. Chemical deposition of thin films of lead selenide. J. Electrochem. Soc., 111 (1964), p. 42.

155. Mulik, R.N., Rotti, C.B., More, B.M., Sutrave, D.S., Shanane, G.S., Garadkar, K.M., Deshmukh, L.P. and Hankara, P.P. Polycrystalline lead selenide thin films: growth from solution solution and properties. Indian J. Pure Appl. Phys., 34 (1996), p. 903.

156. Grozdanov, I., Najdoski, M. and Dey, S.K. A simple solution growth technique for PbSe thin films. Mater. Lett., 38 (1999), p. 28.

157. Kanniainen, T., Lindroos, S., Ihanus, J. and Leskelä, M. Growth of strongly oriented lead sulfide by successive ionic layer adsorption and reaction (SILAR) technique. J. Mater. Chem., 6 (1996), p. 161.

158. Kanniainen, T., Lindroos, S., Resch, R., Leskelä, M., Friedbacher, G. and Grasserbauer, M. Structural and topographical studies of SILAR-grown highly oriented PbS thin films. Mat. Res. Bull., 35 (2000) p.1045.

159. Kanniainen, T., Lindroos, S., Ihanus, J. and Leskelä, M. Growth of lead selenide thin films by successive ionic layer adsorption and reaction (SILAR) technique. J. Mater. Chem., 6 (1996), p. 938.

160. Li, C.P., McCann, P.J. and Fang, X.M. Strain relaxation in PbSnSe and PbSe/PbSnSe layers grown by liquid-phase epitaxy on (100)-oriented silicon. J. Cryst. Growth, 208 (2000), p. 423.

161. Berchenko, M.A. and Belyaev, A.I. Precipitation of selenides and tellurides from aqueous solution. Russ. J. Inorg. Chem., 15 (1970), p. 1034.

162. Skrabek, E.A. Thermoelectric energy conversion. In: Kirk-Othmer Encyclopedia of Chemical Technology, 4th ed. Vol. 23. John Wiley & Sons, New York, 1997. p. 1027.

163. Dhere, N.G. Appropriate materials and preparation techniques for polycrystalline-thin-film thermophotovoltaic cells. AIP Conf. Proc., 401 (1997), p. 432.

164. Gorer, S. and Hodes, G. Quantum size effects in the study of chemical solution deposition mechanisms of semiconductor films. J. Phys. Chem., 98 (1994), p. 5338.

165. Li, L., Qu, L., Wang, L., Lu, R., Peng, X., Zhao, Y. and Li, T. Preparation and characterization of quantum-sized PbS grown in amphiphilic oligomer langmuir-blodgett monolayers. Langmuir, 13 (1997), p. 6183.

166. Salata, O., Dobson, P., Hull, P. and Hutchison, J. Fabrication of PbS nanoparticles embedded in a polymer film by a gas-aerosol reactive electrostatic deposition technique. Adv. Mat. 6 (1994), p. 772.

167. Bauer, G. and Clemens, H. Physics and applications of IV–VI compound quantum well and superlattice structures. Semicond. Sci. Technol., 5 (1990), p. S122.

168. Moss, T.S. Lead salt photoconductors. Proc. IRE, 43 (1955), p. 1869.

169. Espevik, S., Wu, C-H and Bube, R.H. Mechanism of photoconductivity in chemically deposited lead sulfide layers. J. Appl. Phys., 42 (1971), p. 3513.

170. www.arraydetectors.com, usa.hamamatsu.com, www.calsensors.com, www.nepcorp.com

171. Norton, P. Infrared image sensors. Opt. Eng., 30 (1991), p. 1649.

172. Humphrey, J.N. Optimum Utilization of lead sulfide infrared detectors under diverse operating conditions. Appl. Opt., 4 (1965), p. 665.

173. Blount, G.H., Preis, M.K., Yamada, R.T. and Bube, R.H. Photoconductive properties of chemically deposited PbS with dielectric overcoatings. J. Appl. Phys., 46 (1975), p. 3489.

174. Johnson, T.H., Cozine, H.T. and McLean, B.N. Lead selenide detectors for ambient temperature operation. Appl. Opt., 4 (1965), p. 693.

175. U.S. Patent 5275839, Method of sensitizing lead salt detectors. 1994. Smith, T.W.

176. Niemelä, P. On-line measurements of oil contaminats in water by filter-based infrared analyzers. Doctoral thesis. Espoo: Technical Research Centre of Finland, 1994. VTT Publications 208. 110 p. + app. 3 p.

177. Koh, W., Kutner, W., Jones, M.T. and Kadish, K.M. An improved holder for the electrochemical quartz crystal microbalance and its cyclic voltammetry characteristics. Electroanalysis, 5 (1993), p. 209.

178. Feng, H., Laverty, S.J., Maguire, P., Molloy, J. and Meenan, B.J. Electrochemically reduced polycrystalline tin oxide thin films. Surface analysis and electroplated copper adhesion. J. Electrochem. Soc., 143 (1996), p. 2048.

179. Waldo, R.A. An iteration procedure to calculate film compositions and thicknesses in electron-probe microanalysis. Microbeam Anal., (1988), p. 310.

180. Dennison, S. and Webster, S. An electrochemical and optical microscopic study of the reduction of $HTeO_3^+$ in aqueous acid solution. J. Electroanal. Chem., 314 (1991), p. 207.

181. Gabe D.R. The role of hydrogen in metal electrodeposition processes. J. Appl. Electrochem., 27 (1997), p. 908.

182. Sorenson, T.A., Lister, T.E., Huang, B.M. and Stickney, J.L. A comparison of atomic layers formed by electrodeposition of selenium and tellurium. Scanning tunneling microscopy studies on Au(100) and Au(111). J. Electrochem. Soc., 146 (1999), p. 1019.

183. Schroder, D.K., Semiconductor Materials and Devices Characterization, John Wiley & Sons, 1998, New York, p. 43.

184. Cândea, R.M., Dâdârlat, D., Turcu, R. and Indrea, E. Properties of PbSe films prepared by chemical anorganic deposition. Phys. Stat. Sol., (a) 90 (1985), p. K91.

Author(s)
  Saloniemi, Heini

Title

Electrodeposition of PbS, PbSe and PbTe thin films

Abstract

Lead chalcogenides (PbS, PbSe, PbTe) are narrow band gap semiconductors which are largely used in infrared applications. In the present study lead chalcogenide thin films were deposited electrochemically from aqueous solutions. Two different electrodeposition methods were used; PbSe and PbTe thin films were prepared at constant potential while PbS was deposited by cycling the potential.

Chemical and physical properties of the films were examined by various techniques, and their electrical properties were studied as well. PbSe and PbS thin films were found to be stoichiometric whereas PbTe thin films contained an excess of Te. The films contained water as an impurity. All the films had polycrystalline, randomly oriented cubic structure. After annealing the films showed p-type conductivity. The annealing at 100 °C did not affect much the resistivities of PbS and PbTe which remained between 0.5–10 Ω cm but the resistivity of PbSe films increased to 1–60 kΩ cm. All films showed IR activity.

Electrodeposition mechanisms of PbSe, PbTe and PbS thin films and electrochemistry of the related precursors were studied by means of the electrochemical quartz crystal microbalance (EQCM) combined with cyclic voltammetry. Both film growth and EQCM studies showed that the electrodeposition of PbSe and PbTe occurs by the induced codeposition mechanism, where Se (or Te) is deposited first and induces the reduction of lead ions to form PbSe (or PbTe) so that this occurs at more positive potential than where lead alone would be deposited. Electrodeposition of PbS, on the other hand, turned out to be complicated including several simultaneous processes.